Available online at www.sciencedirect.com
SCIENCE DIRECT®
Coordination Chemistry Reviews 238–239 (2003) 143–166
COORDINATION CHEMISTRY REVIEWS
www.elsevier.com/locate/ccr

Electronic spectroscopy and photoreactivity in transition metal complexes

Chantal Daniel *

Laboratoire de Chimie Quantique, UMR 7551 CNRS/Université Louis Pasteur, 4 Rue Blaise Pascal 67000 Strasbourg, France

Received 9 May 2002; accepted 11 October 2002

Contents

Abbreviations: CASPT2, complete active space perturbation theory 2nd order; CASSCF, complete active space self consistent field; CI, configuration interaction; DFT, density functional theory; Δ-SCF, delta-self consistent field; EOM-CCSD, equation of motion coupled cluster single double; MC-SCF, multiconfiguration self consistent field; MP2, Moller Plesset 2nd order; MR-CI, multi reference configuration interaction; MS-CASPT2, multi state CASPT2; RASSCF, restricted active space SCF; SAC-CI, symmetry adapted cluster-configuration interaction; TD-DFT, time-dependent density functional theory.

* Tel.: +33-390241302; fax: +33-390241389.
E-mail address: daniel@quantix.u-strasbg.fr (C. Daniel).

0010-8545/02/$ - see front matter
PII: S0010-8545(02)00295-3

Abstract

The recent developments in quantum chemistry providing the theoretical tools to determine the properties of transition metal complexes in their electronic excited states are presented. The contrast between the impressive fast evolution of the computational strategies adapted to the treatment of ground state molecular properties and the gradual improvement of the methods that are more specifically turned towards the study of electronic excited states is discussed. Recent applications in transition metal coordination chemistry are selected to outline the degree of methodological maturity in electronic spectroscopy and photo-induced reactivity, illustrating the necessity for a strong interplay between theory and experiment.

Keywords: Electronic spectroscopy; Photoreactivity; Transition metal complexes; Quantum chemistry; Wavepacket dynamics

1. Introduction

A survey through the theoretical literature devoted to transition metal complexes is quite revealing about the actual trends. One finds more and more studies attempting to compute molecular properties as accurately as possible. This feature is not surprising since it can be related to the maturing stage of transition metal chemistry: most of the experimental studies carried out nowadays, pertain—either in the ground state or in excited state—to the synthesis and characterization of elaborate systems or to the elucidation and to the design of quite intricate processes [1–4]. They require from theory calculations with an improved accuracy in conjunction with the ability to treat large systems (eventually by including the solvation sphere or the effects of the environment). The properties that are computed include molecular structures, energies (of reaction, of interaction, of electronic transitions), vibrational frequencies, electric and magnetic properties [5–10]. The development of efficient theories and algorithms combined with the availability of very fast computers (especially when running in parallel) has enabled such computations, although they can remain quite challenging. As far as the reactivity is concerned, it is fair to say that one can now compute relatively easily the energy and the structure of the reactants transition state and products of an organometallic reaction in the gas phase provided that the electronic structure of the systems is free of near degeneracy effects. Some of the methods adapted to the treatment of ground state properties and reactivity such as MP2 (Moller-Plesset 2nd Order) [11,12] or DFT (density functional theory) [13–15] are now easily accessible in 'black box' softwares even though a background in quantum chemistry is necessary to analyze their results. In contrast the highly correlated methods used in the computation of near degeneracy problems need skill and experience, the results depending strongly on the way the calculation is driven. From this point of view the theoretical study of the electronic spectroscopy and photo-induced reactivity in transition metal complexes cannot be performed routinely. This will be illustrated in the computational section, which will include several particularities characterizing this class of molecules.

The UV–vis absorption spectrum of transition metal complexes is characterized by a high density of various electronic excited states (metal-centered, metal-to-ligand-charge-transfer, ligand-to-ligand-charge-transfer, sigma-bond-to-ligand-charge-transfer, intra-ligand, ligand-to-metal-charge-transfer). The presence of electronic states of different nature, localisation, dynamics and reactivity in a limited domain of energy gives unconventional photophysical and photochemical properties to this class of molecules and explains the versatility and the richness of their photochemistry [16,17]. Moreover, these specific properties responsible for the occurrence under irradiation of fundamental physico-chemical processes such as electron/energy transfer, bond breaking or formation, isomerisation, radical formation, and luminescence can be tailored chemically and more recently controlled by shaped laser pulses [18]. However, every rose has its thorn and the price to pay is the complexity of the mechanism that underlies the electronic spectroscopy and the excited state reactivity of this class of molecules. Two contrasting behaviours can be considered: after irradiation the molecular system can either be trapped in long-lived excited states of well defined structure leading to beautiful resolved absorption/emission spectroscopy or can land on a repulsive potential energy surface inducing an extremely fast ligand dissociation on the femtosecond time-scale. The

bipyridine substituted complexes which have been intensively studied over the last 30 years are representative of the first category [19] whereas transition metal carbonyls illustrate the second behaviour [20,21]. Unfortunately, most of the time, the bound and repulsive electronic excited states coexist in a limited domain of energy and may interfere in the Franck-Condon region generating structure-less absorption spectra. The interaction between various electronic states in different regions of the potential energy surfaces leads to critical geometrical structures such as saddle points, conical intersections or local minima. Consequently, the observed response of the molecular system to light is entirely governed by the sequence of many concurrent elementary processes. The development of short time resolved spectroscopy (picosecond–femtosecond timescale) in different domains (resonance Raman, FT-Infra-Red, FT-electron paramagnetic resonance, emission, absorption UV–vis) has contributed to a better understanding of excited states structures and processes that are very fast even at low temperature. However, several fundamental questions still remain to be solved. One important aspect is the differentiation between: (i) chemically active electronic states leading to bond breaking or formation, isomerisation, radical production; and (ii) long-lived excited states involved in the photophysics or subsequent secondary processes such as electron/energy transfer. In this respect the determination of the various channels and time scales of deactivation of the excited molecule is especially important. For this purpose a strong interplay between experiment and theory is mandatory. The first role of the theoretical study is to clarify the electronic structure of the complexes, to determine the low-lying electronic transitions and to assign the observed bands. This is probably the easiest task and several computational methods started to emerge in the 90's able to describe electronic spectroscopy in transition metal complexes with reasonable accuracy (see next section). The second aspect, related to the calculation of accurate multidimensional potential energy surfaces describing the reactivity of electronic excited states, is the bottleneck of the theoretical study. There has been an impressive development in the past 15 years of methods based on the energy gradient formalism and adapted to the description of ground state reactivity [22]. However, only a limited number of approaches can be contemplated to obtain a more or less complete characterization of the shape of several excited states potential energy surfaces. The main difficulty is related to the dimensionality of the problem which cannot be solved exactly due to the large number of nuclear coordinates. This implies a selective choice of a few degrees of freedom in the treatment of the dynamics which has to include several coupled electronic excited states, either non-adiabatically or by spin-orbit.

In the next section devoted to computational methods, various more or less *chemist friendly* strategies will be presented. Solvent effects or other phenomena due to the environment will not be discussed in the present review. The use and difficulties of different methods will be illustrated by selected examples focussing on electronic spectroscopy in Section 3 and excited state reactivity for a variety of prototypes and chemical systems in Section 4.

2. Computational methods

2.1. Electronic spectroscopy

The goal is to obtain accurate transition energies (within 0.10–0.15 eV) and reliable dipole transition moments in order to assign bands located in the UV–vis spectral domain of energy in various transition metal complexes. The size of the molecular system, its symmetry and the density of states as well as the saturation of the metal centre d shells or the metal–ligand interactions will generate particular difficulties. The choice of the method will be a compromise taking into account the following factors: (i) the feasibility and computational cost; (ii) the validity of some approximations; (iii) the desired level of accuracy; (iv) the control that can be performed on the analysis of the results. Four types of methods based on different mathematical formalisms are available for treating electronic spectroscopy in transition metal complexes: (i) the DFT such as the delta-self-consistent field (Δ-SCF) [23–28] and time-dependent DFT (TD-DFT) [29–32]; (ii) the variational approaches such as the self-consistent-field (SCF) [33,34], configuration interaction (CI) [35–38], multi configuration SCF (MC-SCF) [39–41], multireference CI (MR-CI) [40,42]; (iii) the cluster expansion methods such as the equation of motion coupled cluster single double (EOM-CCSD) [43–47], the symmetry adapted cluster CI (SAC-CI) [48–50]; (iv) the single state (SS) or

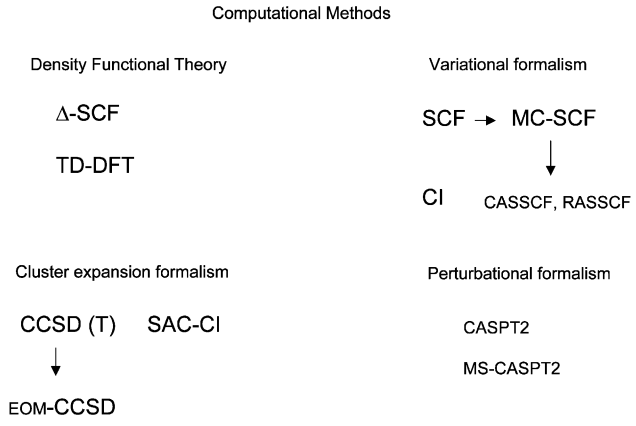

Scheme 1.

multistate (MS) 2nd order perturbational approaches applied to zeroth-order variational wavefunctions and so-called SS-CASPT2 [51–53] and MS-CASPT2 [54]. Most of the methods discussed in the present review are present in the quantum chemical software: MOLCAS [55], GAUSSIAN [56], MOLPRO [57], TURBOMOLE [58], ACESII [59], ADF [60], HONDO [61] (Scheme 1).

2.1.1. Density functional based methods

The optical spectra of transition metal complexes have been interpreted by means of DFT methods for a longtime. The ancestor of DFT the so-called Xα method was used for the MnO_4^- anion, a crucial test case analysed as early as 1970 with satisfactory accuracy on the transition energies [62]. However, the Kohn–Sham orbitals calculated within the DFT formalism describe the electronic ground state in a single determinant scheme. While this method was well established for the ground state and the lowest states, within a symmetry class, from its early days its extension to excited state descriptions is still in development. The first option proposed in 1977 by Ziegler and Baerends [63] within the framework of the time-independent formalism and generalized in 1994 by Daul [64] (so-called Δ-SCF method) is based on symmetry-dictated combinations of determinants able to evaluate in a non-ambiguous way the space and spin multiplets. This approach lacks a formal foundations and relies on the presence of a point symmetry group in the metal centre environment assuring a totally symmetric electron density. It has been applied with success to a variety of highly symmetric molecules [64]. However, several limitations make this approach only accessible to experts in the subject [65]. Indeed, apart from the symmetry conditions the presence of redundant determinants may induce non-negligible errors on the energies. Moreover, configuration mixing other than that dictated by symmetry considerations would have to be handled *a posteriori* in a complicated scheme. In the presence of closely spaced multiplets of the same symmetry, the method will become nearly unworkable. The occasional need to calculate bi-electronic integrals to avoid redundancy may be a drawback as well as convergence to broken symmetry solutions or the number of separate SCF cycles having to be performed for each state.

An alternative to the time-independent DFT method is the so-called time-dependent DFT (TD-DFT). This method based on the linear response theory is the subject of recent and promising theoretical developments [65–67]. The treatment of molecular properties by means of the linear response of the charge density to an applied field is based on a well founded formalism that allows direct computation of polarisabilities, excitation energies and oscillator strengths within the framework of the DFT. Only excitations corresponding to linear combinations of singly excited determinants are included as in single excitation configuration interaction (CIS) but taking into account additional electronic correlation effects. However, the use of approximate exchange-correlation functionals with incorrect asymptotic behaviour may lead to dramatic errors in the case of the TD-DFT method for two main reasons [67]: (i) the most polarisable part of the charge density is at large r; (ii) the asymptotic behaviour of the exchange-correlation potential v_{xc} determines the ionization threshold. The accuracy of the response calculation is very sensitive to the approximation made for v_{xc} as well as to its repercussion on its derivative $\partial v_{xc}/\partial\rho$ (derivative discontinuity in the bulk region). Due to an underestimation of the attractive character of the exchange-correlation potential the charge density will be too diffuse. Consequently the ionisation threshold will be systematically too low with a dramatic effect on high excitation energies and polarisabilities which will be overestimated. Moreover, excitation involving a substantial change in the charge density such as charge transfer states will be described with difficulty by conventional functionals. In spite of these drawbacks the TD-DFT approach remains a computationally simple and efficient method able to treat practical problems in a reasonable time scale at a low cost when compared with highly correlated ab initio methods [68–73]. For medium size molecules or transition metal complexes TD-DFT results have been shown to be competitive with the highest level ab initio approaches but cases where current exchange-correlation functionals dramatically fail are known to exist [74,75]. This recent method is in constant evolution with the aim at improving not only the functionals themselves but also their derivative behaviour in the bulk region for a better description of various types of excited electronic states and of the highest part of the absorption spectrum. In particular exchange-correlation potentials constructed from ab initio densities or including charge transfer corrections should largely contribute to the improvement of the method [76,77].

The calculated dipole transition moments are very sensitive to the quality of the calculation, namely the basis sets and the functional used [78]. Obviously they rely on the hypothesis that DFT excited states are well defined, an assumption which is not always true as explained above. Some functionals have been found to be more sensitive to the basis set quality than others.

2.1.2. Variational approaches

The few attempts at describing excited states in transition metal complexes within the Restricted Hartree Fock (RHF) formalism were rapidly abandoned due to the computational difficulties (convergence of the low-lying states in the open-shell formalism) and theoretical deficiencies (inherent lack of electronic correlation, coherent treatment of states of different

multiplicities and d shell occupations). Most of the time the assignment of the absorption spectra was only qualitative with a systematic underestimation of the metal-centred states transition energies (0.5–1.25 eV in systems such as $[Co(CN)_6]^{3-}$, $Cr(CO)_6$, $[Co(CN)_5(OH)]^{3-}$ [79] and 1.05–1.25 eV in $FeCp_2$ [80]). The simplest and most straightforward method to deal with correlation energy errors is the CI approach where the single determinant HF wave function is extended to a wave function composed of a linear combination of many determinants in which the coefficients are variationally optimized. The first CI based studies of the electronic spectroscopy of transition metal complexes were performed in the late 70's on the series $TiCl_4$, VCl_4, VCl_4^+ taking into account the singly excited configurations [81] and on $Cr(CO)_5$ where single and double excitations were applied on the basis of HF optimized molecular orbitals [82]. In the first case all transitions energies were overestimated by 2.0–3.0 eV whereas in the second study the $^1A_1 \rightarrow {}^1E$ transition was underestimated by 1.0 eV. The error on the transition energies in $TiCl_4$ falls to 0.5–1.5 eV when applying a multi-reference CI scheme where double excitations are performed in a selected reference space of configurations (MRD-CI) [83]. Within the CI formalism the configuration mixing is introduced (multi-determinantal approach) but the predetermined reference set of molecular orbitals is not reoptimized for the different electronic states. However, most of the time and especially in transition metal complexes strong correlation effects affect the electron density. Therefore, it is necessary to optimize the molecular orbitals according to a multi-configurational scheme including static electronic correlation effects which describe the interaction between two electrons in a pair at large separation space. The so-called MC-SCF method and its extension CASSCF (complete active space SCF) [84,85] or RASSCF (restricted active space SCF) [86] methods have their origin in this fundamental problem. These methods provide zero-order wave functions used as references in subsequent CI, MR-CI or MS-CASPT2 calculations which take into account the dynamical correlation effects describing the interaction between two electrons at short inter-electronic distance (so-called cusp region). Obviously the MC-SCF approach is even more crucial in excited state calculations where electronic state mixing and dramatic changes of electron density during the excitation have to be taken into account. The large variation in the number of d electrons pairs among the various electronic states is one major difficulty when correlated methods are applied to transition metal complexes. The most widely used MC-SCF method is the CASSCF based on a partitioning of the occupied molecular orbitals into subsets corresponding to how they are used to build the wave function. The problem is reduced to the partition into sets of active and inactive orbitals and to a selection of correlated electrons. This discriminating strategy based on the physics and chemistry of the study includes all configuration state functions (CSF's) which are generated by distributing the active electrons among the active orbitals in all possible ways consistent with the spin and the symmetry of the wave function. In practical applications where the number of configurations may exceed 10^6 and the size of the active space may vary between 2e2a (where two electrons are correlated into two active orbitals) and 16e16a (where 16 electrons are correlated into 16 active orbitals) such a partitioning is not straightforward. The validity of the subsequent MR-CI or MS-CASPT2 treatments depends entirely on the quality of the CASSCF wave function. This strategy is not easily automated and cannot be used as a black-box. Most of the time the orbitals are optimized for the average energy of a number of excited states large enough to include the electronic spectrum of interest. This procedure avoids root inversions as well as convergence problems and leads to a set of orthogonal wave functions of given spin and symmetry and to transition densities of reasonable accuracy used in properties calculation (dipole transition moments). The transition energy accuracy is obtained by the addition of the remaining correlation effects by means of MRCI or MS-CASPT2 calculations. If the active space can be chosen large enough, according to the physico-chemical aspect of the problem, results of high accuracy will be produced by the CASSCF/CI procedure where the configuration selection scheme on the top of the CASSCF wave function is performed by single and double replacement out of either a single reference (CI) or multi-reference space (MRCI). The spectroscopy of $HMn(CO)_5$ illustrates the quality of such calculations on middle size transition metal complexes for which the error on the calculated transition energies does not exceed 0.25 eV for the low-lying electronic states [87]. However, the slow convergence of the method, the size of which increases dramatically with the number of references and the default of size-extensivity leading to incorrect scaling of the energy with the number of correlated electrons are very limiting for a general use of the MR-CI formalism in non-trivial applications of electronic spectroscopy in large transition metal complexes.

2.1.3. Second order perturbational approach

An alternative to the fully variational approach depicted above is a mixed procedure where a multi-configurational variational method is used to build a zero-order wavefunction supplemented by a 2nd order perturbational treatment of the dynamic correlation effects. The so-called CASPT2 and its multistate extension MS-CASPT2 methods [51–54] are size-extensive and give very accurate transition energies providing that

the variational wave function is suitable at describing correctly the physics involved in the spectroscopy of the system under study''. Otherwise the perturbational treatment is no longer valid due to the presence of intruder states interacting with the reference space and not included at the zero-order level. This leads to an erratic behaviour of the perturbation and to transition energies out of range by more than 2.0 eV. In these non-trivial cases either a level-shift technique has to be applied with care (weak intruder states) [88] or the CASSCF active space has to be increased (strong intruder states) as illustrated by the theoretical study of the spectroscopy of $Mn_2(CO)_{10}$ [89] or $HRe(CO)_5$ [90].

2.1.4. Cluster expansion methods

The cluster expansion methods are based on an excitation operator which transforms an approximate wave function into the exact one according to the exponential ansatz

$$\Psi = \exp(T)|0\rangle \quad (1)$$

where T is a sum of single- to N-particle excitation operators (coupled-cluster theory) [91–93] or of symmetry adapted single- to N-particle excitation operators (symmetry adapted cluster theory) [94]. The simplest truncation of T is to the 2nd Order where the single and double excitations are included in the cluster expansion (CCSD [95] or SAC) based on the HF single determinant $|0\rangle$. When electron correlation effects are dominated by pair effects these methods recover 90–95% of the exact correlation energy if the wave function is described by a dominant closed-shell determinant. The remaining correlation effects due to higher excitations are estimated by approximate methods like in the CCSD(T) approach [96] where the triple excitations are included perturbationally. These methods based on a separated electronic pair approach in which pair clusters are used to describe the correlation between two electrons are size-extensive by definition and independent of the choice of reference orbitals. However, these methods which converge efficiently are hardly generalized to multi-reference starting wave functions. Consequently a number of approximations has to be made which may destroy the size-extensitivity. As far as the excited states and associated properties are concerned, two cluster expansion based methods, developed originally for open-shell situations, have been proposed. The first one, so-called SAC-CI method [48–50] supposes that the major part of electron correlation in the closed-shell ground state is transferable to the excited states since the excitation of interest involves only one and/or two electrons. These transferable dynamical correlation effects are expressed through an exponential operator and a linear operator is used to represent the non-transferable state-specific correlation effects such as quasi-degeneracy's. The absorption spectrum of $TiCl_4$ has been reinvestigated on the basis of this method leading to a perfect agreement with experimental data and a new assignment with an accuracy of the order of 0.15 eV [83]. In the CC based methods, so-called equation-of-motion CCSD (EOM-CCSD) [43–47] ionization potentials, electron affinities and excitation energies are obtained directly from the equation of motion operating on the ground state wave function. This approach, characterized by an unambiguous treatment of excited states where the only choices are the atomic basis sets and the excitation level of the operators is very demanding computationally. It has been applied to only one transition metal complex, namely $FeCl_4^-$ leading to promising results for charge transfer transitions from the $^6A_1$ ground state [97]. A recent workable extension is the so-called extended similarity transformed EOM-CCSD (extended-STEOM-CC) [98]. A first transformation is performed based on the ground state CCSD while a second transformation uses information concerning ionized and attached states obtained from EOM-CCSD ionization potentials and electron affinities. This method (STEOM-CCSD) applied to the transition metal complexes $TiCl_4$, $Ni(CO)_4$ and MnO_4^- [98] yields improved results compared to EOM-CCSD methods with an accuracy very similar to the one obtained at the SAC-CI level for $TiCl_4^-$ [83]. A good description of the ground and ionized states is crucial in this approach and further modifications of the theoretical framework are still required for highly correlated ground states and multi-reference cases.

2.2. Potential energy surfaces

The concept of potential energy surfaces (PES) is the central aspect of the understanding of chemical/photochemical reactions mechanism, the quantum nuclear description of the nuclear motion being determined by the shape of the PES. In photochemical mechanisms we are concerned with reaction paths on ground and excited state PES which can be determined according to the procedures developed for chemical reactivity. The new problem in photo-induced mechanisms is the complicated landscape of the PES characterized by the presence of a variety of critical geometries such as minima, transition states, high-order saddle points, avoided crossings, conical intersections resulting from non-adiabatic interactions between N-dimensional PES.

Within the Born-Oppenheimer (BO) approximation justified by the slow motion of the nuclei as compared to the one of the electrons, the adiabatic PES are obtained by calculating the electronic energy and wave functions for a series of fixed nuclear geometries. Electronic spectroscopy and photochemical reactions involve transitions between two or more PES in the critical regions where the nature of the electronic wave function may

change rapidly as a function of the nuclear displacement. The efficiency of the transition is governed by the non-zero interaction kinetic matrix elements, the BO approximation being no longer valid. For a given atomic basis set the computational method used to solve the electronic problem has to be flexible enough to characterize correctly different regions of the molecular PES at the same level of accuracy. An inadequate wave function would result in a biased description of the different regions and such computed PES would not reproduce the exact BO potentials.

2.2.1. Methods

One of the most significant advances made in applied quantum chemistry in the past 20 years is the development of computationally workable schemes based on the analytical energy derivatives able to determine stationary points, transition states, high-order saddle points and conical intersections on multidimensional PES [22]. The determination of equilibrium geometries, transition states and reaction paths on ground state potentials has become almost a routine at many levels of calculation (SCF, MP2, DFT, MC-SCF, CCSD, CI) for molecular systems of chemical interest [99,100]. The availability of reliable and efficient analytic energy gradient procedures (1st and 2nd derivative) for the search of various critical points on several interacting complex surfaces at a high correlated level (CASSCF, CCSD(T) and it's extension EOM-CCSD, MR-CI) will have a significant impact in the theoretical study of transition metal photo-reactivity. Indeed, although reaction paths are uniquely defined in any coordinate system they cannot be determined unambiguously without the knowledge of reference points on the PES from which the analytical energy derivation procedure may start. Unfortunately the derivative formulation for highly correlated wave functions is very complex and if analytical first derivatives are available for the standard methods 2nd derivatives calculations are even more complicated. In coupled cluster as in MC-SCF based methods the computational requirement of the gradient step is usually significantly less demanding than the evaluation of the wave function. However, while the storage of the atomic orbitals effective density matrix is the bottleneck in the CC type calculations restricting this method to small molecules, the gradient-MCSCF based methods show serious convergence problems at the electronic level making the geometry optimization of electronic excited states very delicate. Moreover the coherence of the CSF's expansion of the MC-SCF in the different regions of the PES as well as the stability of the set of active molecular orbitals will be guaranteed only with large state-averaged MC-SCF active spaces not tractable for large molecules. The effort required to optimize MR-CI (SD) wave functions scales roughly as the number of references times the effort for a single reference CI (SD) wave function of the same size in term of active orbitals [100]. This computational effort limits the size of the studied molecules to less than ten atoms mainly hydrogen and 2nd row atoms. Moreover, this non-extensive method truncated with respect to the excitation level has difficulties at providing a correct wave function at dissociation. Density functional methods are competitive with the above traditional wave functions methods for numerous applications among them the computation of ground state PES. A few applications to transition metal photochemistry have been proposed on the basis of the Δ-SCF approach implying several approximations on the excited states reaction paths definition by symmetry constraints not always appropriate in a 'coordinate driving' scheme [101]. Excited-state gradients have been recently implemented in DFT for various functionals, the feasibility of the approach having been tested for small molecules only [102]. The recent development of a multi-component density functional theory treating the fully coupled system of electrons and nuclei within a very complicated time-dependent formalism should open the field to a variety of excited states problems including photochemistry [103,104].

2.2.2. Strategy

The mathematical and computational machinery for structure optimization is based on various algorithms, the complexity of which depends on the desired accuracy at the electronic level. The application of these methods to photochemical problems raises serious practical difficulties as illustrated above. The computation of accurate multidimensional PES for several interacting electronic states in transition metal complexes is beyond the actual capabilities. For simple mechanisms involving the electronic ground state interacting with one excited state the global structure of the low-energy part of the PES can be visualized within a 3-D cross section plotting the energy on a grid while the critical points (minima, transition states, conical intersections) are fully optimized using rigorous ab initio correlated methods (MC-SCF). This strategy has been applied with success to a number of organic photochemical reactions for which the number of electronic states involved in the mechanism is modest while the multidimensional character of the PES is essential due to the flexibility of this class of molecules [105–109]. In contrast the central metal atom in transition metal complexes induces blocking effect and most of the time only a few degrees of freedom participate in the photochemical reaction. However, the high density of electronic states which characterizes the absorption spectrum generates very complicated PES involving several singlet and triplet states (8–12 in standard molecules) in the UV–vis domain of energy. A systematic investigation of the full PES being practically intractable the study of photochemical processes in transition metal complexes is generally based

on several approximations: (i) the nuclear dimensionality is reduced to $N \leq 2$; (ii) the reaction path is approximated by metal–ligand bond elongation coordinates; (iii) the highest symmetry is retained along the reaction path; (iv) a limited evaluation of geometrical relaxation effects in excited states is performed. These approximations are based on the following criteria: (i) the observed or calculated structural deformations on going from the electronic ground state to the excited state; (ii) the observed or calculated structural deformations on going from the reactant to the products; (iii) the hierarchy in time of the various elementary processes participating in the photochemical behaviour. The validity of these approximations is checked on the basis of the observables directly comparable with the experimental data such as the bond dissociation energies, the main spectral features or the time-scales of primary reactions as illustrated in the applications section. In contrast, the electronic problem is treated by means of the most accurate quantum chemical methods in order to get a semi-quantitative characterization of electronic spectroscopy in the Franck-Condon region and a correct description of the dissociative processes. The analysis of the main topological characteristics of the PES represented by contour maps (2-D) or profiles (1-D) of the potentials $V(q_i)$ is the first step towards a qualitative understanding of the photochemical mechanisms. The next step rests on the investigation of the excited states dynamics.

2.3. Wave packet dynamics

The photo-induced reactivity in transition metal complexes is characterized by the occurrence of several fragmentation schemes originating in complicated mechanisms where several electronic states, reaction paths and elementary processes such as direct/indirect dissociation, internal conversion or intersystem crossing may operate. The simulation of the dynamics following the photon absorption is not an easy task and two different situations have to be considered: (i) ultra-fast direct dissociation from the absorbing state itself (adiabatic process); (ii) indirect dissociation via internal conversion or intersystem crossing (non-adiabatic process). A third case, not contemplated here would be the trapping in longlifetime excited states followed by emission to the electronic ground state, inhibiting reactivity. The motion of the molecular system under the influence of the potential is determined by the equations of dynamics. Consequently, the shape of the computed PES entirely governs this motion. Since, as explained in the previous section, several approximations have to be made at the level of the dimensionality of the PES it is very important to define clearly the initial conditions of the simulation and to estimate the hierarchy in time of the various elementary processes involved in the photochemical reactivity. In conventional photochemical experiments with long pulse duration and narrow frequency resolution only a few near-degenerate electronic states are directly populated. The energy is not in large excess and to a first approximation the reaction paths can be defined by the metal–ligand bond elongation coordinates corresponding to the observed photochemical reactions. In the case of very fast dissociative processes (10 fs–1 ps) the system should not deviate significantly from this 'pseudo minimum energy path' and the many other vibrational degrees of freedom can be frozen. Moreover, there is no justification without any knowledge of the time scale of the dissociation for a full geometry optimization along the excited state reaction paths as necessary in ground state reactivity studies. Typically one or two coordinates corresponding to the bond elongations describing the observed photochemical reactions (CO loss or metal–R, R = H, alkyl, metal, X) are selected for building 1D or 2D PES, the other degrees of freedom being frozen to the Franck-Condon geometry [110,111](Scheme 2).

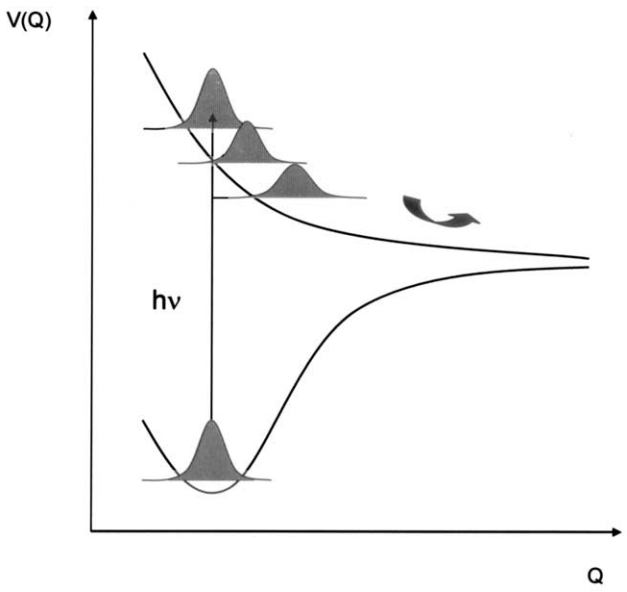

Scheme 2.

The quantum dynamics of photodissociation processes can be performed within the time-independent or time-dependent framework [112]. In the time-dependent picture used in the applications presented in the next section the time-dependent Schrödinger equation is solved

$$i\hbar \frac{\partial}{\partial t}\ \varphi_e(t) = \hat{H}_e \varphi_e(t) \qquad (2)$$

where $\varphi_e(t)$ is a wave packet (coherent superposition of all stationary eigenstates in the electronic excited state)

evolving on the excited electronic state e potential. In order to describe the initial absorption, followed by direct dissociation, it is assumed that the initial vibrational state ϕ_{gi} in the electronic ground state multiplied by the transition dipole function μ_{eg} is instantaneously promoted by the photon to the upper electronic state (Scheme 2). This initial wave packet, which is not an eigenstate of $\hat{H}_e$, starts to move under its action. The advantage of this approach is that the motion of the wave packet, the centre of which remains close to a classical trajectory, can be followed in real time. The motion of the wave packet from the Franck-Condon region to the exit channel is described by the autocorrelation function

$$S(t) = \langle \varphi_e(0) | \varphi_e(t) \rangle \tag{3}$$

given by the overlap of the evolving wave packet with the initial wave packet at $t = 0$. The absorption spectrum is calculated as the Fourier Transform of the autocorrelation function

$$\sigma_{tot}(\omega) \alpha \omega \int_{-\infty}^{+\infty} dt S(t) e^{iEt\hbar} \tag{4}$$

where $E = E_i + \hbar\omega$ [113]. Wave packet calculations lead to the time-scale and probabilities of dissociation and to the branching ratio between concurrent primary processes occurring from a single electronic excited state. In the cases of indirect dissociative processes involving non-adiabatic transitions (jumps between different PES) a set of coupled time-dependent Schrödinger equations has to be solved

$$i\hbar \frac{\partial}{\partial t} \varphi_e(t) = \hat{H}_e \varphi_e(t) + V_{ee'} \varphi_{e'}(t)$$

$$i\hbar \frac{\partial}{\partial t} \varphi_{e'}(t) = \hat{H}_{e'} \varphi_{e'}(t) + V_{e'e} \varphi_e(t) \tag{6}$$

with the same initial conditions as above but in a different basis, the so-called diabatic where the original adiabatic PES have been transformed in order to minimize the kinetic coupling between them and to introduce potential coupling terms $V_{ee'}$. This strategy is very efficient simultaneously to describe intersystem crossings and internal conversions, important processes in photo-induced reactivity in transition metal complexes.

2.4. Relativistic effects

Molecules that contain heavy elements (in particular 5d transition metals) play an important role in the photochemistry and photophysics of coordination compounds for their luminescent properties as well as for their implication in catalysis and energy/electron transfer processes. Whereas molecular properties and the electronic spectroscopy of light molecules can be studied in a non-relativistic quantum chemical model, one has to consider the theory of relativity when dealing with elements that belong to the lower region of the periodic table. As far as transition metal complexes are concerned one has to distinguish between different manifestations of relativity. One of the most important effects in electronic spectroscopy and photoreactivity is spin-orbit coupling. Indeed the coupling between the spin and orbital momentum breaks the strict spin selection rules deduced from non-relativistic quantum theory. The influence of this coupling between singlet and triplet electronic states on the spectra of transition metal complexes may be profound. The potential energy surfaces associated with the triplet states which are degenerate in the non-relativistic approximation, are split according to the symmetry rules of the molecular point double group representation. Consequently, new critical geometries such as avoided crossing or conical intersection where non-radiative transitions may take place efficiently will appear leading to complicated shapes drastically modifying the photo-reactivity. Other important but not directly observable manifestations of relativity are the mass velocity correction and the Darwin correction. These terms lead to the so-called *relativistic contraction* of the s- and p-shells and to the *relativistic expansion* of the d- and f-shells. A chemical consequence of this is for instance a destabilisation of the 5d shells with respect to the 3d shells in transition metals.

In most quantum chemistry codes, relativity is either not treated or treated by the means of relativistic effective potentials. At a less approximate level efficient scalar relativistic (SR) methods are available such as the Douglas–Kroll–Hess (DKH) approach which aims at decoupling the large and small components of the Dirac–Fock equations [114–116] or of the Dirac–Kohn–Sham equations [117,118] as in PARAGAUSS [119]. An alternative method used in the ADF program [60,119] is the zeroth-order regular approximation (ZORA) based on an effective and transparent way treating relativistic effects of valence shells of heavy atom systems by means of a two-component variational approach [121,120,122]. All these methods have been applied essentially to electronic ground state molecular properties and reactivity. In the calculations based on relativistic effective potentials the core electrons are replaced by an effective potential that is fitted to the solution of atomic relativistic calculations and only valence electrons are explicitly handled in the quantum chemical calculation. This approach is in line with the chemist's view that valence electrons of an element mainly determine its chemical behaviour. Several libraries of relativistic effective core potentials (ECP) using the frozen-core approximation with associated

optimized valence basis sets are available nowadays to perform efficient electronic structure calculations on large molecular systems. Among them the pseudo-potential methods [123–130] handling valence nodeless pseudo-orbitals and the model potentials such as AIMP (ab initio model potential) [131–134] dealing with node-showing valence orbitals are very popular for transition metal calculations. This economical method is very efficient for the study of electronic spectroscopy in transition metal complexes [89,90].

However, several efficient computational codes based on the relativistic analogue of the Hartree–Fock method, the Dirac–Fock (Breit) method have been developed in the past decade able to treat relativistic and electronic correlation effects at the same level with the usual correlated methods of quantum chemistry (DIRAC [135], MOLFDIR [136], UTCHEM [137–140], BERTHA [141], DREAMS [142]). The computational cost of the fully-relativistic methods is not comparable to standard quantum chemical calculations and only a few applications dealing with coordination compound spectroscopy can be cited. These include the d–d spectra of transition metal fluorides CoF_6^{2-}, RhF_6^{2-} and IrF_6^{2-} with MOLFDIR [143]. It has been shown for instance that non-dynamical correlation effects arising from low-lying charge-transfer states are found to be the most important in CoF_6^{2-}, while spin-orbit effects dominate in IrF_6^{2-}.

One fundamental aspect in understanding the photochemical behaviour of transition metal complexes is the role of the triplet states on the photoreactivity. The calculation of spin-orbit coupling (SOC) effects is mandatory and should be performed in connection with highly correlated methods. The zero-field splitting of triplet molecular states can be calculated by the means of perturbation theory when the spin-orbit effects are much smaller than other electronic interactions [144]. When the SOC treatment is required on the same footing with other interactions (heavy elements) it is necessary to go beyond the perturbation theory using a variational approach based on a spin-orbit Hamiltonian. An illustration is given by the previous example of transition metal fluorides [143] where the perturbative model to calculate the spin-orbit coupling gives good results which compare rather well with experimental data in the Co complex. In contrast the splitting of the quartets of IrF_6^{2-} is overestimated and a fully relativistic Configuration Interaction approach is necessary for treating this molecule.

An extension of the combined DFT/MRCI method to spin-orbit effects has recently been proposed recently which is able to evaluate spin-dependent properties for excited electronic states in large molecular organic systems [145]. To our knowledge this promising method has never been applied to the electronic spectroscopy of transition metal complexes.

2.5. Basis set effects

Despite the fact that exact atomic orbitals are inaccessible, atomic orbitals represent the most suitable set of functions for expanding molecular orbitals in the LCAO (linear combination of atomic orbitals) formalism. In nearly all ab initio calculations reported today basis sets of contracted Gaussians are used. There are a number of choices regarding the atomic orbital exponents and contraction coefficients. Obviously in order to be adapted to excited states calculations in molecular systems containing transition metal atoms, the basis sets have to be constructed to take into account several aspects: (i) the various electronic configurations of the metal centre in the excited molecule; (ii) the level of calculation; (iii) the description of the outer region of the charge density cloud. Basis sets required for an accurate description of ground state properties may be inadequate for the investigation of the electronic spectroscopy in the same molecule. Highly correlated methods such as MC-SCF, MR-CI or CCSD(T) will need more complete basis sets than single determinantal methods of the HF type. In order to describe correctly the outer region of the charge density cloud, diffuse functions will be necessary in the case of Rydberg states [87]. Polarization functions (basis functions with L-quantum numbers higher than the valence L-quantum number) may be important to describe significant displacements of electron density as in metal-to-ligand-charge-transfer states for instance. The difficulty is to find the best compromise between the computational cost and the accuracy. In this respect the scheme of contraction will be very important. For 2nd and 3rd row transition metal complexes the use of ECP including relativistic effects and associated valence basis sets is a good compromise. For first-row transition metal complexes atomic natural orbitals (ANO) [146,147] constructed by averaging the corresponding density matrix over several electronic configurations (ground state, valence excited states, positive and negative ions) are required to obtain good structural properties, ionization potentials, electron affinity and transition energies. Finally as in ground state molecular calculations the choice of the basis sets associated with the surrounding ligands has to be coherent with the basis sets chosen for the metal centre, especially for a good description of metal-to-ligand-, sigma-bond-to-ligand- or ligand-to-metal charge-transfer states. The lower limit as far as the basis sets quality is concerned for standard correlated calculations (CASSCF, MR-CI, MS-CASPT2 or TD-DFT) in middle size transition metal complexes is at least Double-Zeta with polarization functions for the 2nd row atoms and Triple-Zeta for the metal atoms. Highly correlated methods such as the CCSD theory are even more demanding in term of basis sets quality and this is one of the limiting steps for further applications in the field

of transition metal complexes electronic spectroscopy [98]. Systematic investigations of the basis set effects on the electronic spectroscopy of α-diimine and bipyridine transition metal carbonyls either at the CASSCF/MS-CASPT2 or at the TD-DFT level seem to indicate that the differences in the transition energies never exceed 1000 cm^{-1} (in the worst case of conjugated systems) and accounts for a few hundred of cm^{-1} in most cases. This effect is very small as compared to the choice of the CASSCF active space or of the functional in TD-DFT. The use of similar quality Slater basis functions instead of Gaussian basis sets may be more advantageous from the computational point of view leading to similar accuracy.

3. Electronic spectroscopy

The calculated electronic transitions reported in Tables 1 and 2 for MnO_4^-, $TiCl_4$, $FeCp_2$, $Ni(CO)_4$, $Cr(CO)_6$ and $Mn_2(CO)_{10}$ illustrate the evolution over the past 30 years of the computational strategies developed for the treatment of electronic spectroscopy in transition metal complexes. The details of the one electron excitations in the principal configuration which describes the transitions are not given for the sake of clarity. Indeed, inherent conflicting assignments in term of molecular orbitals between density functional based methods and ab initio methods would throw reader into confusion.

3.1. *Prototype systems:* MnO_4^-, *$TiCl_4$, $FeCp_2$*

The correct theoretical treatment of the absorption spectrum of MnO_4^- has been a long standing problem and is still a challenge for quantum chemists. The low-lying transitions correspond to charge transfer from non-bonding oxygen orbitals to anti bonding metal-oxygen d orbitals and are characterized by strong mixing between close-lying configurations. Moreover, important correlation effects involve the bonding metal–oxygen orbitals lying below the non-bonding oxygen orbitals. Consequently a CASSCF/MS-CASPT2 multiconfigurational treatment would need a rather large unworkable active space to describe both the one-electron excitations and the correlation effects at the zero order. The electronic spectroscopy of this molecule has been investigated in the past by SCF-Xα [62], SCF [184] and CI(SD) [148] and more recently by ΔSCF [149], TD-DFT [70,150] and cluster expansions

Table 1
Calculated electronic allowed transition energies (in eV) of MnO_4^-, $TiCl_4$ and $FeCp_2$ by different methods

	SCF-Xα [a]	SCF [b]	CI(S) [c](SD)	CI (MR-D) [d]	ΔSCF (DFT) [e]	TD-DFT [f]	SAC-CI [g]	EOM-CCSD (Ext-STEOM) [h]	Exp [i]
MnO_4^-									
1^1T_2	2.3	3.09	(2.6)		2.71	2.63–2.82	2.57	2.24 (1.92)	2.27
2^1T_2	3.3	3.42	(4.2)		4.02	3.60–3.89	3.58	3.67 (3.08)	3.47
3^1T_2	4.7	4.24	(4.5)		4.22	4.41–4.74	3.72	3.60 (3.51)	3.99
4^1T_2	5.3	6.29	(6.0)		5.70	5.46–5.84	5.82	5.80 (5.48)	5.45
$TiCl_4$									
1^1T_2			6.2	5.08			4.42	4.64 (4.44)	4.43
2^1T_2			6.7	6.69			5.22	5.24 (4.99)	
3^1T_2			7.1	6.93			5.53	5.49 (5.44)	5.38
4^1T_2			–	6.95			5.74	5.63 (5.53)	
7^1T_2			7.8	8.18			7.20	(6.58)	7.07
8^1T_2			8.3	8.79			7.72	(6.90)	7.39
$FeCp_2$									
1^1E_{2g}		1.66	2.65		2.87	1.74–2.97			2.98
1^1E_{1g}		2.72	5.76		–	2.27–3.09			2.70
2^1E_{1g}		1.77	3.34		3.48	3.07–3.62			3.82

[a] Ref. [62].
[b] SCF MnO_4^- [184] and $FeCp_2$ [80].
[c] Single (S) and double (SD) excitations in the CI for MnO_4^-, $TiCl_4$ [148] [81] and $FeCp_2$ [80].
[d] Multireference CI including double excitations $TiCl_4$ [151].
[e] DFT (ΔSCF) MnO_4^- [149] and $FeCp_2$ [25].
[f] The transition energies are functional dependent MnO_4^- [150,70] and $FeCp_2$ [150].
[g] SAC-CI $TiCl_4$[83]MnO_4^-[151].
[h] EOM-CC [98]and Extended Similarity Transformed in parenthesis.
[i] Experimental spectrum from Ref. [185–187], for MnO_4^-, $TiCl_4$ and $FeCp_2$, respectively.

methods such as SAC-CI [151] or EOM-CCSD [98]. Surprisingly the crude but parameterized SCF-Xα method was able to lead as early as 1971 to a reasonable description of the spectrum of MnO_4^- using only a few minutes of computer time as compared to the 10 h of computer time on similar computers required by the SCF and CI(SD) methods at that time. The Hartree Fock based methods (SCF, CI(SD)) lead to important discrepancies due to an incorrect description of the metal–oxygen bonding and to a non-balanced description of the electronic excited states with respect to the ground state. The best agreement between the experimental spectrum and the calculated transition energies is obtained on the basis of the TD-DFT method with a systematic overestimation of the transition energies varying between 0 and 24% depending on the quality of the functional. In addition the cluster expansion based methods such as SAC-CI and EOM-CCSD approaches may either over or under estimate the transition energies by no more than 13% (SAC-CI) and 10% (EOM-CCSD). The extended similarity transformed-EOM method, economical extension of the rather expensive EOM-CCSD approach leads to disappointing results due to its single reference character. An important aspect is the strong dependence of the TD-DFT results on the type of functionals as discussed in Ref. [70] where several functionals have been tested for various systems among them MnO_4^-. The use of the ΔSCF approach, based on orbital replacement energies and separately optimized excited states orbitals does not include the multi-configurational character of the problem and leads to important quantitative differences with respect to the TD-DFT method which works on ground state orbitals. As a consequence not only the transition energies but also the assignment, proposed by the density functional based methods, differs significantly. All method reported in Table 1 agree upon the assignment of the first band of MnO_4^- to the $1t_1 \rightarrow 2e$ excitation. The analysis of the upper part of the absorption spectrum is much debated, the TD-DFT method leading to a different assignment than ΔSCF or cluster expansion based methods for the second and third bands and to the same assignment as the SAC-CI for the fourth band. None of these methods is perfect for treating the electronic spectroscopy of this non-standard molecule and it is difficult to push the comparison too far at the present time.

$TiCl_4$ which has been the subject of several theoretical studies [81,83,98] is among the simplest transition metal complexes (d^0 system). The electronic correlation effects are considered to be minor in this molecule, the description of which, in contrast to MnO_4^- does not need highly correlated methods at the zero-order. The electronic spectroscopy of $TiCl_4$ has been investigated by means of CI and cluster expansion based methods. The lowest part of the absorption spectrum is described by valence excitations corresponding mainly to charge transfer from the p(Cl) non-bonding and metal–ligand bonding orbitals to metal–ligand anti bonding orbitals. The transition energies are systematically overestimated by the CI calculations based on an HF wave function (12–40% in the case of the CI(S) and 15–27% with the CI(MR-D) procedure). These results illustrate the poor capacity of the CI at reproducing correct transition energies even at the multi-reference level including double excitations as long as a unique set of molecular orbitals optimized for the electronic ground state is used for the calculation of the electronic excited states. In contrast the SAC-CI and EOM-CCSD results are comparable and reproduce perfectly the transition energies leading to the assignment of the lowest part of the absorption spectrum without any ambiguity. The lowest observed band at 4.43 eV corresponds to a nearly pure ligand to metal charge transfer state ($2t_1 \rightarrow 3e$) whereas three states of mixed characters contribute to the second band at 5.38 eV.

The last example reported in Table 1 concerns $FeCp_2$ one of the metallocenes which has been the subject of numerous experimental and theoretical studies for their photophysical and magnetic properties. The absorption spectrum of Ferrocene is characterized by two Metal Centred bands around 2.7 and 3.8 eV the first one being composed of two transitions to the $^1E_{2g}$ and 1^1E_{1g} states [152]. The SCF and SCF/CI(S) calculations lead to dramatic errors on the transition energies and an incorrect relative order of the three low-lying E_{2g} and E_{1g} singlet excited states. The density functional based methods and especially the ΔSCF method reproduces the observed bands rather well and gives a correct assignment of the experimental spectrum. However, large deviations on the transition energies are obtained with the TD-DFT method depending on the functionals as was the case for MnO_4^-. In general the prediction of excitation energies is reasonable for low-lying states as long as a functional with correct asymptotic behaviour is used but erratic behaviours may occur for specific cases. For a further discussion on the impact of functionals on the excited states calculations in a series of metal complexes see Ref. [70].

3.2. Transition metal carbonyls: $Ni(CO)_4$, $Cr(CO)_6$, $Mn_2(CO)_{10}$

Transition metal carbonyls constitute a very important class of complexes in laser chemistry as reactive precursors of catalytic processes, substitution reactions, chemical vapour deposition of thin films or layers on surfaces. They are among the most reactive transition metal complexes and their electronic structure has long been a matter of considerable interest stimulating theoretical research. Even though their experimental spectra have been known since the early 1970s relatively

Table 2
Calculated electronic allowed transition energies (in eV) of $Ni(CO)_4$, $Cr(CO)_6$ and $Mn_2(CO)_{10}$ by different methods

	ΔSCF [a] (DFT)	TD-DFT [b]	CASSCF/CASPT2 [c]	SAC-CI [d]	EOM-CCSD (Ext-STEOM) [e]	Exp. [f]
$Ni(CO)_4$						
1^1T_2		4.7	4.34	4.79	4.93 (4.24)	4.5–4.6
2^1T_2		4.82	5.22	5.51	5.35 (4.74)	5.4
3^1T_2		5.37	5.57	5.76	5.76 (5.03)	(5.2, 5.5)
4^1T_2		5.84	6.28	–	6.39 (5.99)	6.0
5^1T_2		6.74	6.97	–		
$Cr(CO)_6$						
1^1T_{1u}	5.6	4.19 (3.91)	4.54–4.11			4.43
2^1T_{1u}	6.5	5.76 (5.37)	5.07–5.2			5.41
$Mn_2(CO)_{10}$						
1^1E_1	3.62	3.44	3.29			3.31
1^1B_2	3.42	4.01	3.43			3.69

[a] DFT (ΔSCF) $Cr(CO)_6$ [158] and $Mn_2(CO)_{10}$ [161].
[b] TD-DFT $Ni(CO)_4$ [70] $Cr(CO)_6$ [68] and $Mn_2(CO)_{10}$ [70].
[c] CASSCF/CASPT2 $Ni(CO)_4$ [154], $Cr(CO)_6$ [154] and $Mn_2(CO)_{10}$ [89].
[d] Ref. [151].
[e] Extended similarity transformed EOM [98].
[f] Experimental absorption spectra from Ref. [153,152,155] for $Ni(CO)_4$, $Cr(CO)_6$ and $Mn_2(CO)_{10}$, respectively.

little attention has been given to the electronic spectroscopy of the molecules reported in Table 2, namely $Ni(CO)_4$, $Cr(CO)_6$ and $Mn_2(CO)_{10}$. A fundamental aspect of the theoretical study is related to the electronic correlation effects which are already very important at the electronic ground state level for a good description of the metal–CO bonding in these molecules. The results reported in Table 2 were obtained by means of correlated methods able to describe correctly the dπ–pπ backbonding interaction in this class of molecules. The experimental spectrum in gas phase of $Ni(CO)_4$ (a d^{10} system) exhibits three bands attributed to MLCT $^1A_1 \rightarrow {}^1T_2$ transitions [153]. The TD-DFT [70], CASPT2 [154], SAC-CI [151] and EOM-CCSD [98] approaches give rise to three allowed transitions in the energy range 4.0–6.5 eV in agreement with experiment leading to a reasonable assignment. The deviations on the transition energies never exceed 7%. Again the assignment of the upper bands in term of one electron excitations in the principal configurations is quite sensitive to the level of calculation and is still controversies.

The spectrum of $Cr(CO)_6$ (a d^6 system) is dominated by two very intense absorption bands assigned to MLCT $^1A_{1g} \rightarrow {}^1T_{1u}$ transitions and by low-lying shoulders originally attributed to weak MC transitions [152]. This assignment was confirmed by semi-empirical INDO/S CI [153] and SCF calculations [156,157]. The more recent studies reported in Table 2 and based on ΔSCF [158], TD-DFT [68] and CASSCF/CASPT2 [154] methods reinterpreted the electronic spectrum of $Cr(CO)_6$. According to this new analysis the lowest part of the spectrum does not correspond to MC transitions but rather to orbitally and spin-forbidden MLCT states of low intensity not reported in Table 2 where only the intense bands observed at 4.43 and 5.41 eV are presented. If the TD-DFT and CASPT2 results are in excellent agreement with the experimental values the ΔSCF method overestimates the transition energies by more than 20%. These poor results are attributed to the inability of this approach to account for the configuration mixing which characterizes these two states.

The $Mn_2(CO)_{10}$ prototype for bimetallic transition metal complexes has attracted considerable interest for its photochemical reactivity leading to competitive primary reactions, namely CO loss and homolytic cleavage of the Mn–Mn bond [159]. The quantum yield of these two reactive channels is controlled by the excitation wavelength. The lowest part of the absorption spectrum is characterized by one poorly resolved shoulder at 3.31 eV attributed to the $^1A_1 \rightarrow {}^1E_1$ ($d_\pi \rightarrow \sigma^*_{Mn-Mn}$) transition and one intense band at 3.69 eV assigned to the $^1A_1 \rightarrow a^1B_2$ transition corresponding to the $\sigma_{Mn-Mn} \rightarrow \sigma^*_{Mn-Mn}$ excitation (σ_{Mn-Mn} and σ^*_{Mn-Mn} are the metal–metal bonding and its antibonding counterpart orbitals). This early assignment by Gray et al. [160] was confirmed recently by the CASSCF/CASPT2 [89] and TD-DFT [70] calculations, the results of which are in excellent agreement with experiment (see Table 2). In contrast the ΔSCF results which have been shown to be extremely sensitive to the geometry agree

Table 3
Comparison between the calculated and experimental spectra of plastocyanin, nitrite reductase, NiP, NiTBP, NiPc

	Calculated [a]	Experimental [b]
Plastocyanin		
$\sigma^*(Cu–S)\rightarrow\pi^*(Cu–S)$	0.55	0.63
$3d_{z^2}(Cu)\rightarrow\pi^*(Cu–S)$ [c]	1.46	1.35
$3d_{yz}(Cu)\rightarrow\pi^*(Cu–S)$ [c]	1.62	1.60
$3d_{xz}(Cu)\rightarrow\pi^*(Cu–S)$ [c]	1.58	1.74
$\pi(Cu–S)\rightarrow\pi^*(Cu–S)$ [d]	1.96	2.09
$\sigma(Cu–S)\rightarrow\pi^*(Cu–S)$ [d]	2.75	2.67
Nitrite Reductase		
$\pi^*(Cu–S)\rightarrow\sigma^*(Cu–S)$	0.55	0.7
$3d_{z^2}(Cu)\rightarrow\sigma^*(Cu–S)$	1.54	1.49
$3d_{yz}(Cu)\rightarrow\sigma^*(Cu–S)$	1.61	1.69
$3d_{xz}(Cu)\rightarrow\sigma^*(Cu–S)$	1.73	1.86
$\pi(Cu–S)\rightarrow\sigma^*(Cu–S)$	1.97	2.19
$\sigma(Cu–S)\rightarrow\sigma^*(Cu–S)$	2.81	2.74
NiP		
1^1E_u	2.40 (0.0052)	2.28 (Q)
2^1E_u	3.23 (1.0214)	3.11 (B)
NiPz		
1^1E_u	2.42 (0.2692)	2.11 (Q)
2^1E_u	3.00 (0.0226)	3.30 (Sh)
4^1E_u	3.51 (0.1465)	3.65 (B)
NiTBP		
1^1E_u	2.08 (0.3130)	2.01 (Q)
2^1E_u	2.95 (0.7144)	3.00 (B)
3^1E_u	3.10 (0.5354)	3.22
6^1E_u	3.62 (0.0627)	3.60
NiPc		
1^1E_u	1.97 (0.6520)	1.90 (Q)
4^1E_u	3.20 (0.3396)	~3.40 (B1)
7^1E_u	3.61 (0.2254)	
8^1E_u	3.85 (0.4650)	3.79 (B2)

The transition energies are given in eV.
[a] Calculated spectra for plastocyanin and nitrite reductase [163] and for the nickel tetrapyrrole series [72].
[b] Experimental spectra for plastocyanin and nitrite reductase [164] and for the nickel tetrapyrrole series: NiPz, NiTBP [72] and NiPc, NiP [166,165].
[c] Although these excitations formally should be classified as ligand field transitions they involve a significant movement of charge from the copper into SCys.
[d] Purely Charge Transfer States

with the characters of the two bands but differ in their relative ordering [161].

This previous section dedicated to the electronic spectroscopy of prototype systems gave an illustration of the evolution of the different computational strategies in the past 30 years. Obviously one goal of the theoretical study is to assign and reproduce the resolved absorption spectra with accuracy also one desires to predict and to understand the electronic spectroscopy of systems of chemical and biological interests at a quantitative level. The next examples based either on CASSCF/CASPT2 or on TD-DFT approaches should give, to the reader, a feeling of what can nowadays be done in this respect.

3.3. Bio-inorganic systems: the blue copper protein and the nickel tetrapyrrole series

In some beautiful recent work by the groups of Pierloot and Roos [162,163] a fairly complete understanding of the relation between the electronic spectra and structure of the mononuclear copper–cysteinate proteins was proposed. This theoretical work is based on DFT geometry optimizations of several blue copper protein models from $[Cu(NH_3)_2(SH)(SH_2)^+]^+$ to $[Cu(imidazole)_2(SCH_3)(S(CH_3)_2)^+]^+$ the structures of which are compared to the crystal structures of plastocyanin and nitrite reductase. The effect on the spectra of the protein environment has been simulated by a single point-charge model. The CASSCF/CASPT2 calculated electronic spectra of the $[Cu(imidazole)(SH(SH_2)^+]$ model using the crystal structure but with CASPT2 optimized $Cu–S_{Cystein}$ and $Cu–S_{Methionin}$ bonds distances reproduce the experimental absorption spectra [164] of the blue copper protein plastocyanin and nitrite reductase with an error of less than 0.22 eV as illustrated in Table 3 and according to the assignment of the authors [163].

The key point in this type of study is the choice of the model systems the structure of which should be very close to the real systems. Indeed, the change in geometry has a dramatic effect on the electronic structure itself and on the electronic spectroscopy. It has been shown that both the trigonal and tetragonal structures of the blue copper protein models are rather similar (nearly tetrahedral). Therefore, some proteins stabilize the trigonal structure (e.g. plastocyanin) whereas others stabilize the tetragonal structure (e.g. nitrite reductase). The electronic spectra of blue copper proteins are well characterized and have been recorded by several spectroscopic techniques. The spectra show a prominent peak centered at 2.08 eV in plastocyanin and 2.19 eV in nitrite reductase responsible for the blue color and a weak band around 1.5 eV. All the transitons reported in Table 3 correspond to excitations either to the $\pi^*(Cu–S_{Cys})$ (plastocyanin) or to the $\sigma^*(Cu–S_{Cys})$ (nitrite reductase) orbitals strongly delocalized onto S_{Cys}. The lowest part of the spectra is attributed to ligand field (LF) states by the authors, the upper part being characterized by the presence of high-lying Charge Transfer states from the $\pi(Cu–S_{Cys})$ or the $\sigma(Cu–S_{Cys})$ orbitals.

The second example reported in Table 3 is a complete TD-DFT study of the electronic spectroscopy of the nickel tetrapyrrole series [72], NiP, NiPz, NiTBP and NiPc (P = porphyrins, Pz = porphyrazines, TBP = tetrabenzoporphyrins, Pc = phthalocyanines). The optical spectra of metal complexes with the most representative

tetrapyrrole ligands have been the subject of numerous experimental and semi-empirical studies for more than 50 years. However, little theoretical effort has been expended to explain the dependency of the energetics and intensity of the main UV–vis bands on the macrocycle framework as well as on the central metral atom. For instance Pz, TBP and Pc complexes all exhibit a significant red shift in energy and a intensification relative to the B (Soret) band of the lowest energy $\pi \rightarrow \pi^*$ (Q) band. The aim of recent and complete work published by A. Rosa et al. was to quantify and interpret the main spectral changes along the series NiP → NiPz, NiP → NiTBP, NiP → NiPc.

The absorption spectrum of NiP is characterized by an intense feature corresponding to the B band at 3.11 eV and a very weak Q band at 2.28 eV [165]. The calculated transition energies and oscillator strengths calculated for the two low-lying ^1E_u states agree perfectly with the experimental data and account for the observed Q and B bands. These two states correspond to a 50:50 mixture of two electronic configurations corresponding to $\pi \rightarrow \pi^*$ excitations ($1a_{1u} \rightarrow 5e_g$ and $4a_{2u} \rightarrow 5e_g$).

The visible region of the absorption spectrum of the NiPz complex [72] is dominated by an intense Q band centered at 2.1 eV whereas the UV domain of energy is characterized by a broad band starting at ~3.0 eV with a weak shoulder at 3.3 eV and a pronounced one at 3.65 eV. The transition energies and oscillator strengths reported in Table 3 for NiPz allow the assignment of two low-lying nearly pure ^1E_u states to the Q band ($\pi \rightarrow \pi^*$) whereas the upper B band observed at 3.65 eV and calculated at 3.51 eV is a mixture of several configurations with a non-negligible MLCT character.

The absorption spectrum of NiTBP is dominated by a rather intense Q band centered at 2.01 eV [72]. The near-UV domain of energy is characterized by a narrow Soret (B) band at 3.0 eV followed by two less intense and broader absorptions centered at 3.22 and 3.6 eV. The 1^1E_u calculated at 2.08 eV and responsible for the Q band ($\pi \rightarrow \pi^*$) is nearly pure. The next intense 2^1E_u and 3^1E_u states have mixed character whereas the 6^1E_u state has mainly a pure $\pi \rightarrow \pi^*$ character.

The absorption spectrum of NiPc is characterized by an intense feature in the visible (Q band) at 1.90 eV and an intense B band in the near UV region at 3.79 eV [166]. The 1^1E_u state calculated at 1.97 eV with a very high oscillator strength can be assigned without any ambiguity to the Q band which is nearly pure. The three next states 4^1E_u, 7^1E_u and 8^1E_u calculated at 3.20, 3.61 and 3.85 eV are responsible for the presence of a broad B band in the spectrum of NiPc.

These theoretical results on the nickel tetrapyrrole series agree very well with the experimental data. On the basis of this work an accurate description of the UV–vis absorption spectra recorded either in gas phase (NiPc, NiP) or in solution (NiTBP, NiPz) has been possible. The variation of the Q and B bands energetics and intensities along the series is due to fundamental electronic changes and to the more or less mixed character of the excited states contributing to these bands.

Table 4
CASSCF/CASPT2 and TD-DFT excitation energies (in eV) and assignments of the low-lying electronic transitions of $[Ru(SnH_3)(CH_3)(CO)_2(Me\text{-}DAB)]$ and $[Ru(Cl)(CH_3)(CO)_2(Me\text{-}DAB)]$ [74]

	TD-DFT	CASSCF/CASPT2	Experiment [a]
$Ru(SnH_3)(CH_3)(CO)_2$ (Me-DAB)			
$b^1A'\sigma_{E\text{-}Ru\text{-}E} \rightarrow \pi^*_{DAB}$	2.69	2.55	2.32
$a^1A''4d_{xy} \rightarrow \pi^*_{DAB}$	2.71	2.60	2.78
$c^1A'4d_{xz} \rightarrow \pi^*_{DAB}$	3.42	3.21	3.17
$d^1A'4d_{y^2-z^2} \rightarrow \pi^*_{DAB}$	3.62	3.91	–
$Ru(Cl)(CH_3)(CO)_2$ (Me-DAB) [b]			
$a^1A''4d_{xy} \rightarrow \pi^*_{DAB}$	1.81	2.24	2.17
$b^1A'4d_{xz} \rightarrow \pi^*_{DAB}$	2.03	2.83	2.72
$c^1A'\sigma_{E\text{-}Ru\text{-}E'} \rightarrow \pi^*_{DAB}$	2.91	3.35	3.51
$d^1A'4d_{y^2-z^2} \rightarrow \pi^*_{DAB}$	3.39	3.82	–

[a] See Ref. [74].
[b] The one-electron excitation in the main configuration is given for the CASSCF/CASPT2 calculation. As explained in the text it differs significantly from the TD-DFT assignment for the a^1A'' and b^1A' states.

3.4. Mixed-ligand metal α-diimine carbonyls: $[Ru(E)(E')(CO)_2(iPr\text{-}DAB)]$ ($E = CH_3$, $E' = SnPh_3$ or Cl; iPr-DAB = N,N′-diisopropyl-1,4-diaza-1,3-butadiene)

Transition metal carbonyl–diimine complexes are known for their unconventional photochemical, photophysical and electrochemical properties [167]. The degree of electronic delocalisation over the α-diimine group, the metal centre and the other ligands can be controlled within a series of structurally related compounds or even within the same molecule leading to important spectroscopic and photochemical consequences. The $[Ru(E)(E')(CO)_2(\alpha\text{-diimine})]$ (E, E′ = halide, alkyl, benzyl, metal-fragment; α-diimine = derivatives of 1,4-diaza-1,3-butadiene or 2′2′-bipyridine) complexes which represent an important class of low-valent metal complexes simultaneously containing electron-acceptor ligands and π donors such as halides and/or σ-bounded alkyl or metal-fragment ligands have themselves great potential as luminophores, photosensitizers and visible light photoinitiators of radicals formation. According to their spectroscopic and photochemical properties $[Ru(E)(E')(CO)_2(\alpha\text{-diimine})]$ complexes [168–172] can be classified into two distinct

groups: (i) complexes in which at least one of the E, E′ ligands is an halide; (ii) complexes where E or E′ are either an alkyl group or metal-fragment. On the basis of a recent theoretical and experimental study [74] of the spectra of model and real molecules the absorption UV–vis spectra of a series of $[Ru(E)(E')(CO)_2(i\text{Pr-DAB})]$ ($E = E' = SnPh3$ or Cl; $E = SnPh3$ or Cl, $E' = CH3$) complexes have been analyzed. Remarkably good agreement between the TD-DFT and CASSCF/CASPT2 approaches has been found for the $[Ru(SnH_3)_2(CO)_2(Me\text{-DAB})]$ and $[Ru(SnH_3)(CH_3)(CO)_2(Me\text{-DAB})]$ complexes whereas the two methods lead to different descriptions of the electronic spectroscopy of the halide complexes $[Ru(Cl)(CH_3)(CO)_2(Me\text{-DAB})]$ and $[Ru(Cl)_2(CO)_2(Me\text{-DAB})]$, models for the *i*Pr-DAB and $SnPh_3$ substituted molecules.

The TD-DFT and CASSCF/CASPT2 calculated transition energies as well as the main features of the experimental absorption spectra are reported in Table 4 for $[Ru(SnH_3)(CH_3)(CO)_2(Me\text{-DAB})]$ and $[Ru(Cl)(CH_3)(CO)_2(Me\text{-DAB})]$ prototypes of the two distinct groups (with and without an halide ligand). The calculated transition energies allow an unambiguous assignment of the spectra of the non-halide complexes as illustrated by the values reported for the CH_3/SnH_3 substituted molecule. The lowest energy part of the absorption spectrum (visible) originates in so-called SBLCT (sigma-bond-to-ligand-charge-transfer) electronic transitions that correspond to $\sigma_{E-Ru-E'} \rightarrow \pi^*_{DAB}$ excitations while absorption between 22 250 (2.78eV) and 32 000 (4.0eV) cm^{-1} is due to MLCT transitions corresponding to $4d_{Ru} \rightarrow \pi^*_{DAB}$ excitations. While the agreement between the TD-DFT and CASPT2 is excellent for the non-halide complex, the two approaches lead to different results for the halide substituted molecule. The TD-DFT systematically underestimates the transition energies of $[Ru(Cl)(CH_3)(CO)_2(Me\text{-DAB})]$ predicting a mixed XLCT/MLCT character with the XLCT component being predominant whereas the CASSCF/CASPT2 assign the lowest-energy absorption to MLCT transitions. Dramatic differences were found between characters of the high-lying occupied orbitals ($4d_{Ru}$ in ab initio vs. p_{Cl} in DFT) and of the $\sigma_{E-Ru-E'}$ orbitals describing the bonding as calculated by DFT and CASSCF/CASPT2. A direct comparison is very difficult since in one case (CASSCF) the electronic relaxation is taken into account when going from the ground state to the excited states whereas the single excitations are performed on the basis of a single set of Kohn-Sham orbitals obtained for the ground state density in the DFT approach. Moreover, the electronic correlation effects included in both methods are not equivalent and cannot readily be discussed.

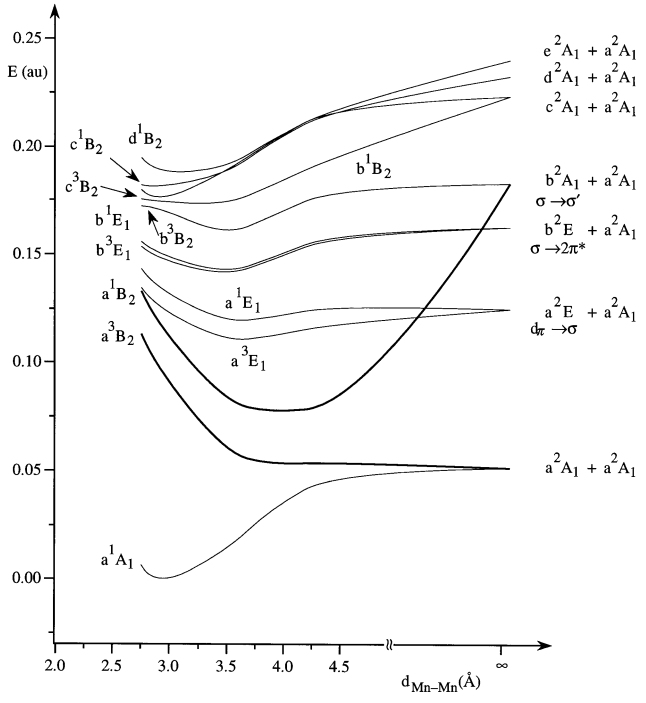

Fig. 1. Potential energy curves for the metal–metal bond homolysis of $Mn_2(CO)_{10}$ obtained by means of the DFT method [173] (reproduced with the permission of the author E.J. Baerends).

4. Excited states reactivity

In order to illustrate the complexity of excited state reactivity in transition metal complexes two selected examples are reported in the next section, namely a DFT study of the photodissociation of $Mn_2(CO)_{10}$ and a CASSCF/MS-CASPT2 investigation of the photochemistry of $[Ru(SnH_3)(CH_3)(CO)_2(Me\text{-DAB})]$. A third example dedicated to the CASSCF/MR-CI study of the photodissociation of $(H)M(CO)_3(H\text{-DAB})$ (M = Mn, Re) will show that despite this apparent complexity invaluable information regarding the photodissociation dynamics can be obtained on the basis of wave packet propagations on selected 2D PES.

4.1. A DFT study of the photodissociation of $Mn_2(CO)_{10}$

The aim of this theoretical work [173] was to propose a qualitative mechanism explaining the occurrence of two primary reactions, namely the Mn–Mn bond homolysis at low energy irradiation (350 nm) and the CO loss at 248 and 193 nm. This study is based on the one-dimensional DSCF potential energy curves (PEC) calculated as a function of the Mn–Mn, Mn–COeq bonds elongations.

As an illustration the computed PEC for the metal–metal bond homolysis are reported in Fig. 1. These PEC have been obtained with the best available functionals at the time of the study, including both Becke's and

Perdew's non-local corrections. The D_{4d} symmetry has been retained along the pseudo reaction path defined as the Mn–Mn bond elongation for which the other bond lengths and the angle $C_{eq}MnMn$ have been optimized at each point using the gradient technique.

This strategy which is entirely justified along a predetermined ground state reaction path is more questionable for excited state reactivity which may occur along dissociative potentials inducing important dynamical effects such as ultra-fast dissociation in the fs time-scale. In such a situation there is no justification for a complete a priori geometry optimization at each point which would suppose that the system has enough time for relaxing along the excited potential. The set of PEC represented in Fig. 1 calculated for the homolytic breaking of the Mn–Mn bond in $Mn_2(CO)_{10}$ and restricted to the symmetry allowed $^{1,3}B_2$ and $^{1,3}E_1$ transitions under the D_{4d} symmetry constraint illustrates the complexity of the excited state reactivity between 0.13 a.u. (350 nm) and 0.24 a.u. (193 nm). In particular the number of curves in this energy range (for clarity, six E_1 states have been omitted by the authors) and their various character make the theoretical analysis very complicated. At a first glance eleven electronic states may participate directly or indirectly to the observed photochemistry. As far as the Mn–Mn bond homolysis is concerned only the low-lying a^1E_1 and a^1B_2 states calculated at the ΔSCF level at 3.62 (345 nm) and 3.42 eV (365 nm), respectively and reordered by means of TD-DFT at 3.44 (363 nm) and 4.01 eV (311 nm) and MS-CASPT2 at 3.29 (379 nm) and 3.43 eV (364 nm) (see Table 2) are accessible by low-energy excitation (350 nm or 3.57 eV) within the theoretical uncertainty. The a^1E_1 which is characterized by a low oscillator strength is weakly bound whereas the a^1B_2 corresponding to the $\sigma_{Mn-Mn} \rightarrow \sigma^*_{Mn-Mn}$ excitation which does absorb strongly shows a shallow minimum at very long Mn–Mn distance (around 4.0 Å). The shape of this potential calculated until 4.5 Å and sketched beyond indicates a considerable weakening of the metal–metal bond but does not show any dissociative character to the ionic species $Mn(CO)_5^+/Mn(CO)_5^-$ as expected. The authors mention an avoided crossing with a lower $^1B_2$ state correlating with the $b^2A_1+a^2A_1$ states at dissociation but not calculated. In this molecule the low-energy photoreactivity, namely the metal–metal bond homolysis should occur through $^1A_1 \rightarrow a^1B_2$ absorption followed by $a^1B_2 \rightarrow a^3B_2$ intersystem crossing within a few tens of ps. This is in contradiction with femtosecond pump/probe experiments which mention an ultra fast process within 100 fs more compatible with a direct dissociation [174]. A clearer picture of the potentials could be obtained nowadays by the TD-DFT procedure using more sophisticated functionals including the asymptotic correction and other corrections taking into account the electronic relaxation in excited states.

4.2. Photodissociation of *[Ru(SnH$_3$)(CH$_3$)(CO)$_2$(Me-DAB)]*

In order to understand the dramatic dependence of the photoreactivity of the [Ru(E)(E′)(CO)$_2$(*i*Pr-DAB)] complexes on the E and E′ ligands (metal fragment, methyl or halide) the CASSCF/MS-CASPT2 PEC describing the Ru–SnH$_3$, Ru–CH$_3$ and Ru–Cl bonds breaking in the model systems [Ru(SnH$_3$)$_2$(CO)$_2$(Me-DAB)], [Ru(SnH$_3$)(CH$_3$)(CO)$_2$(Me-DAB)] and [Ru(CH$_3$)(Cl)(CO)$_2$(Me-DAB)] have been computed [175]. Indeed, if the halide complexes are unreactive even at room temperature the non-halides are photo-

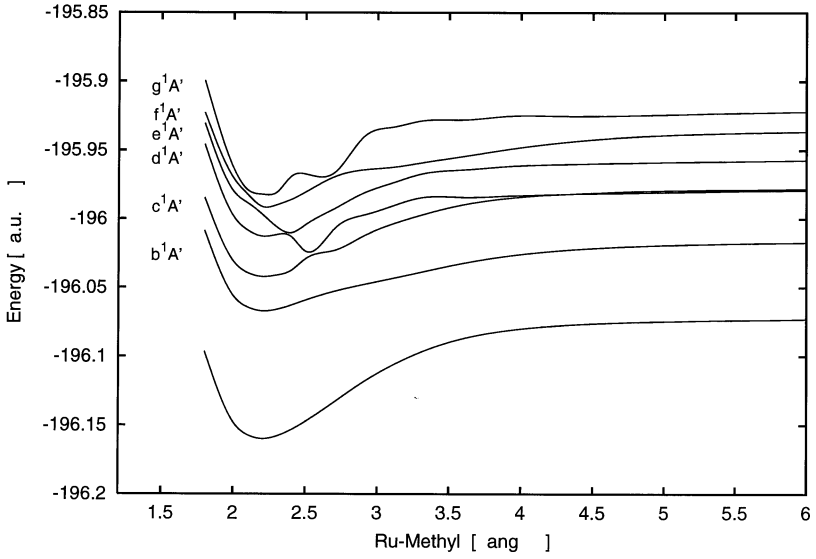

Fig. 2. MS-CASPT2 Potential energy curves for the Ru–methyl bond homolysis of Ru(SnH$_3$)(CH$_3$)(CO)$_2$(Me-DAB) [175].

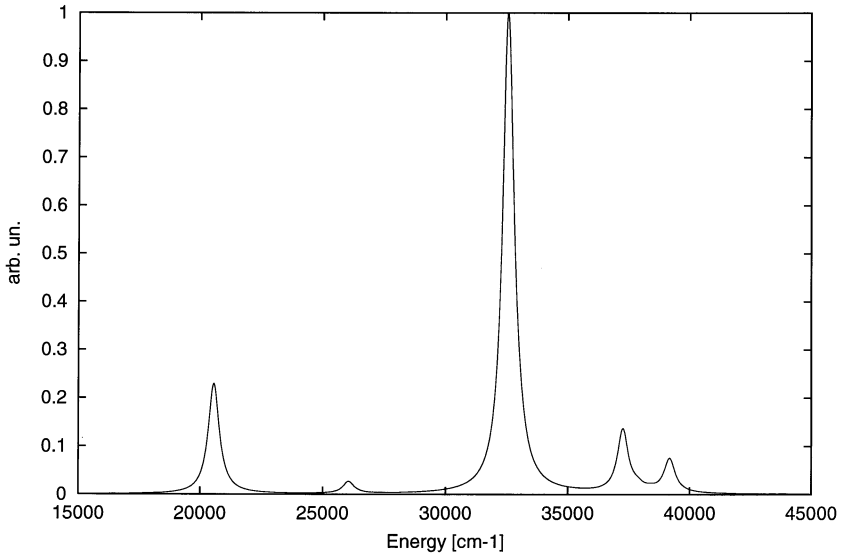

Fig. 3. Theoretical absorption spectrum of $Ru(SnH_3)(CH_3)(CO)_2$(Me-DAB) obtained by Fourier Transform of the autocorrelation function $S(t) = \langle\Psi(t=0)|\Psi(t)\rangle$ [176].

labile leading to the formation of radicals with quantum yields varying between 0.006 and 0.3 involving a rather slow process in the ps to ns time-scale and depending on the axial ligands E and E′. This photoreactivity is wavelength independent and temperature dependent. Fig. 2 represents the set of PEC associated with the low-lying ^{1}A′ excited states of [$Ru(SnH_3)(CH_3)(CO)_2$(Me-DAB)] accessible through visible to far UV irradiation.

Some of these excited states (the d^1A′ and f^1A′) have negligible oscillator strengths whereas only two states the b^1A′ SBLCT state and the c^1A′ MLCT state have significant oscillator strengths absorbing in the visible and near-UV, respectively. To this overcrowded set of PEC three ^{1}A″ curves corresponding to MLCT and SBLCT states of low oscillator strengths have been omitted for clarity. In this example many avoided crossings occur leading to local minima, transition states and double well potentials. The low-lying singlet states are bound and the visible photoreactivity leading to the Ru–CH_3 bond homolysis more likely occurs through an intersystem crossing mechanism to the low-lying dissociative ^{3}SBLCT state in agreement with the time-scale observed experimentally for the methyl substituted complex (ps). The shape of these potential energy curves is responsible for the main features of the absorption spectrum simulated by wave packet propagation and depicted in Fig. 3 [176].

The absorption in the visible around 20 000 cm^{-1} (2.50 eV) is attributed to the low-lying ^{1}SBLCT (b^1A′) state whereas the intense peak around 32 500 cm^{-1} (4.06 eV) is due to the transition to the ^{1}MLCT (d^1A′) state. Several transitions to the upper excited electronic states contribute to the UV and far-UV energy domain of the absorption spectrum beyond 35 000 cm^{-1} (4.37 eV).

4.3. Photodissociation dynamics of M(H)(CO)$_3$(H-DAB) (M = Mn, Re)

The photodissociation dynamics of M(H)$(CO)_3$(H-DAB) (M = Mn, Re), model systems for R$M(CO)_3$(α-diimine) complexes (with M = Mn, Re, R representing a metal fragment or alkyl or halide groups bound to the metal by high-lying σ_{M-R} orbitals) have been investigated in two recent studies [177,178]. The main purpose was to understand the change of photochemical behaviour upon visible irradiation, namely from the CO loss and/or Mn–R bond homolysis to the Re–R bond homolysis and/or emission when going from the first-row to the third-row transition metal complexes [179–183]. Despite the presence of many potentially photoactive low-lying singlet and triplet excited states (nine for the Mn complex and seven for the Re one) it has been shown that only two states, the ^{1}MLCT absorbing state and the ^{3}SBLCT states will control the photochemistry of this class of molecule. As illustrated by the contour plot of the 2D PES associated with these two excited states in both molecules (Fig. 4a and b) the ^{1}MLCT absorbing state itself is dissociative for the CO loss in Mn(H)$(CO)_3$(H-DAB) whereas it is bound in the rhenium analogous.

The dissociative character of the MLCT state in the first-row transition metal complexes is due to the weakening of the Mn–CO_{axial} bond when exciting an electron from the d_{Mn} orbital which is responsible for the dπpπ Mn–CO_{ax} back bonding interaction to the π^*_{DAB} localized on the acceptor group. This effect is less important in the third-row transition metal complexes where the metal–CO_{axial} interaction occurs mainly through the interaction with the diffuse p of the metal. In contrast the ^{3}SBLCT state presents a valley of

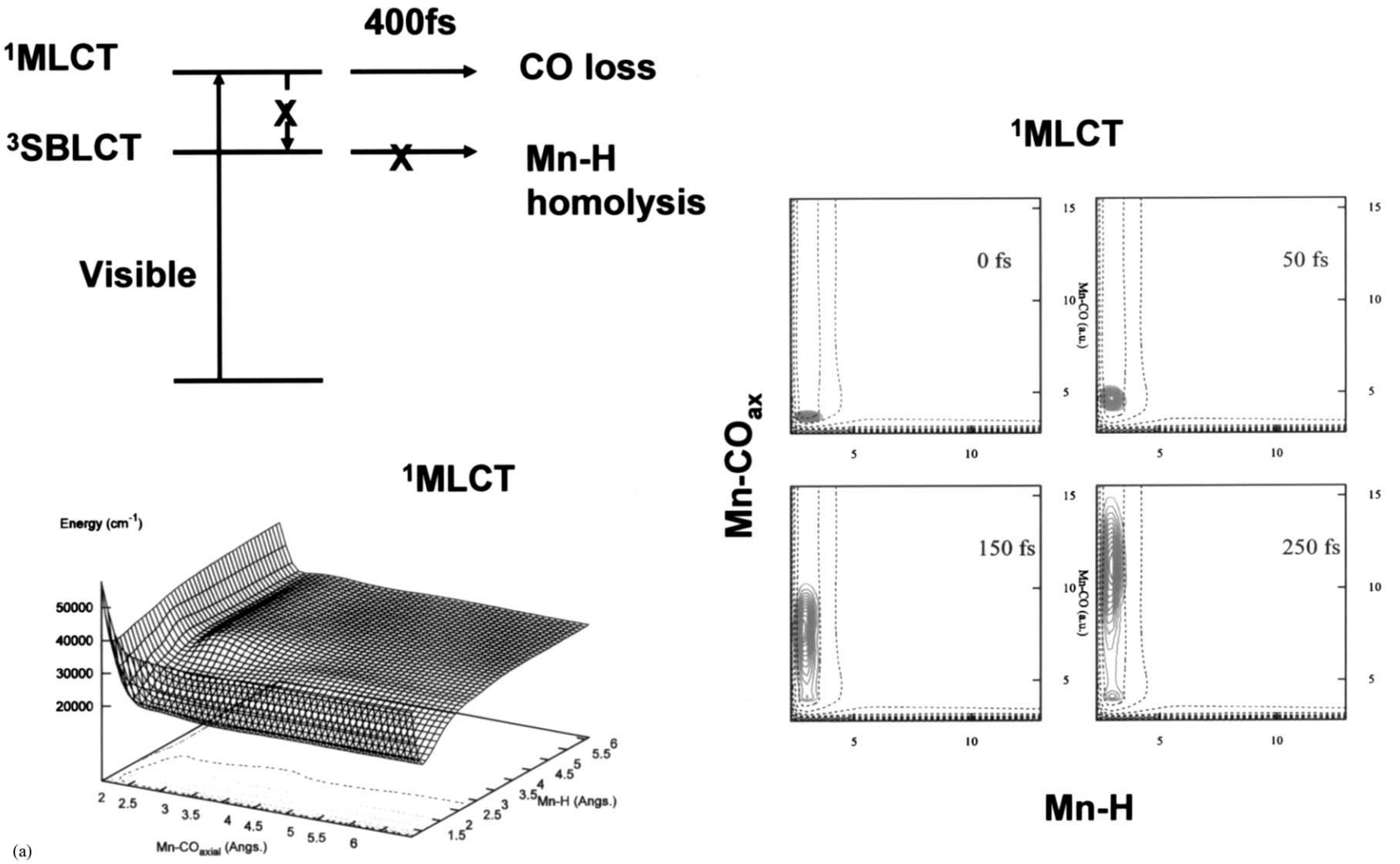

Fig. 4. CASSCF/MR-CI $V_{^1\mathrm{MLCT}}(q_a, q_b)$ potential energy surfaces as a function of the metal–CO_{ax} and metal–hydrogen bond elongation and time evolution of the wave packet $\Psi_{^1\mathrm{MLCT}}(t)$ on the $V_{^1\mathrm{MLCT}}(q_a, q_b)$ potential of the ^{1}MLCT absorbing state of (H)M$(CO)_3$(H-DAB) and proposed mechanism for: (a) M = Mn; and (b) M = Re for M = Re the time-evolution of the $\Psi_{^3\mathrm{SBLCT}}(t)$ on the associated $V_{^3\mathrm{SBLCT}}(q_a, q_b)$ potential is also represented on the right side of Fig. 4b illustrating the ^{1}MLCT → ^{3}SBLCT intersystem-crossing process [177,178].

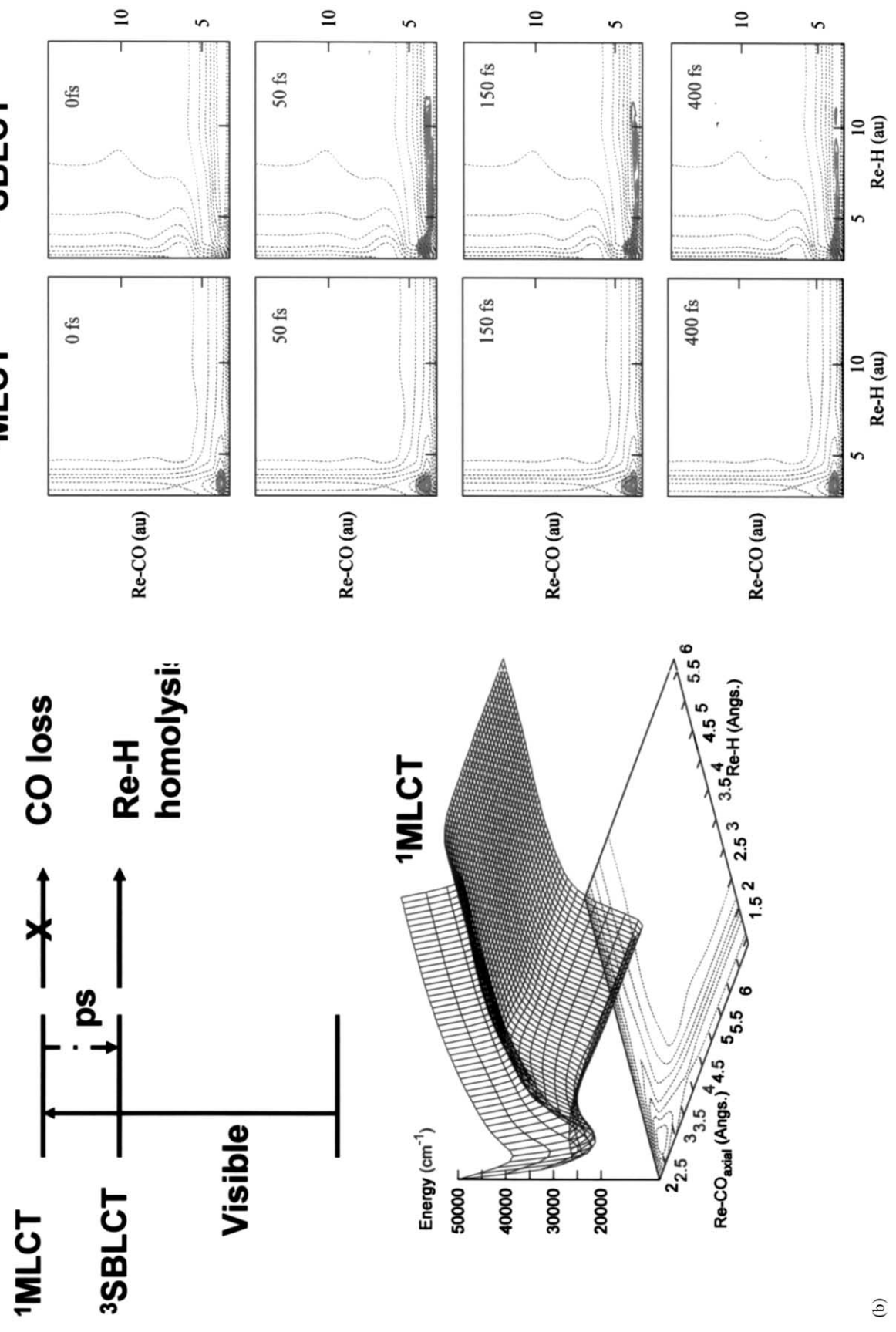

(b)

Fig. 4 (*Continued*)

dissociation for the metal–hydrogen bond breaking in both molecules. Consequently after absorption to the ^{1}MLCT in the visible energy domain $Mn(H)(CO)_3$(H-DAB) will completely dissociate within 450 fs according to an ultra-fast direct dissociative process (Fig. 4a) whereas $Re(H)(CO)_3$(H-DAB) will be trapped in the MLCT bound state (Fig. 4b).

Within the 2D approximation one possibility for the deactivation of $[Re(H)(CO)_3$(H-DAB)]* is via intersystem crossing to the ^{3}SBLCT state as illustrated in Fig. 4b, this potential being repulsive for the Re–H bond homolysis reaction which is observed experimentally. This theoretical study was the first evidence of the MLCT reactivity of the manganese α-diimine complexes observed experimentally and explained why the CO loss is unlikely in the third-row transition metal complexes.

5. Concluding remarks

The theoretical approach to excited state properties was based mainly on a qualitative scheme in terms of molecular orbital analysis until the early 1980s when began an expansion of the electronic correlated methods. The development of efficient theories and algorithms able to take into account the electronic correlation effects and the multi-states problem, combined with a new generation of computers (fast, vector oriented or parallel, with huge memory and storage capacities) has made challenging computations possible. These provided transition energies within 0.15 eV of accuracy even on large molecular systems at different levels of theory based either on wave function or on density functional formalism. However, in this latter case the expertise is not yet sufficient with respect to the ability of the current functionals to describe a variety of excited states and additional validation calculations have to be performed.

With the spectacular development of the very popular Kohn-Sham DFT method in the last decade, ground state chemical properties can be accurately predicted and reactivity interpreted on the basis of a simple and convenient analysis. Recent research devoted to implementation that scales only linearly with the system size opens the route to the treatment of systems with hundreds, may be even thousands of atoms. The solvent effects can be already be taken into account in a number of algorithms and the hybrid methods such as Quantum Mechanics/Molecular Mechanics (QM/MM) bring within reach the treatment of other environment effects on systems of chemical/biological interest. The ground state reactivity can be analyzed in term of a single energy profile along a well defined reaction path characterized by a few critical geometries such as minima or transition states accessible through the standard quantum chemical methods. In contrast the photo-induced reactivity follows very complicated mechanisms involving non-adiabatic processes with jumps between different PES. The bottleneck of the theoretical study is the computation of refined multi-dimensional PES of consistent accuracy in the various potential energy domains (Franck-Condon, Asymptotic region, critical geometries). Alternative methods based on molecular dynamics, so-called 'on the fly', which avoid the computation of such complicated PES cannot be used actually for studying photo-reactivity in transition metal complexes mainly due to the difficulty at converging the energy and it's gradient in the presence of several near-degenerate electronic excited states. On the basis of ab initio two-dimensional PES it is possible to deduce several important photo-physical/photo-chemical properties from wave packet simulations such as the time-scale of photo-dissociation, non-radiative processes such as intersystem crossings. The main features of the absorption spectra or the branching ratio between different primary reactions are also accessible. Within the limit of the theoretical model it is mandatory to perform such simulations in close collaboration with experimentalists. From this point of view the confrontation between the phenomena observed in the femtosecond laser pulse experiments and the results of quantum dynamics is primordial.

Acknowledgements

The author is grateful to Alain Dedieu and Marc Bénard for more than 15 years of advice and stimulating scientific discussions.

References

[1] Organometallics in Organic Synthesis Chem. Rev. Special Issue A. D. Meijere Guest Editor 100 (8) (2000) 2739.
[2] Frontiers Metal-Catalyzed Polymerization Chem. Rev. Special Issue J. A. Gladysz Guest Editor 100 (4) (2000) 1167.
[3] M.T. Pope, A. Müller (Eds.), Polyoxometalate Chemistry From Topology via Self-Assembly to Applications, Kluwer Academic Publishers, 2001.
[4] I. Haiduc, F.T. Edelman (Eds.), Supramolecular Organometallic Chemistry, Wiley-VCH, 1999.
[5] Computational Transition Metal Chemistry Chem. Rev. Special Issue E.R. Davidson Guest Editor 100 (2) (2000) 351–818.
[6] M.M. Rohmer, M. Bénard, A. Strich, J.P. Malrieu, J. Am. Chem. Soc. 123 (2001) 9126.
[7] K. Morokuma, Phil. Trans. Roy. Soc. London A 360 (2002) 1149.
[8] T. Kerdcharoen, K. Morokuma, Chem. Phys. Lett. 355 (2002) 257.
[9] D.V. Denbel, T. Ziegler, Organometallics 21 (2002) 1603.
[10] E.J. Baerends, G. Ricciarddi, A. Rosa, Coord. Chem. Rev. 230 (2002) 5.
[11] C. Møller, M.S. Plesset, Phys. Rev. 46 (1934) 618.

[12] J.A. Pople, R. Seeger, R. Krishnan, Int. J. Quant. Chem. Symp. 11 (1977) 149.
[13] P. Hohenberg, W. Kohn, Phys. Rev. 136 (1964) B864.
[14] W. Kohn, L.J. Sham, Phys. Rev. 140 (1965) A1133.
[15] J.A. Pople, P.M.W. Gill, B.G. Johnson, Chem. Phys. Lett. 199 (1992) 557.
[16] 13th International Symposium on Photochemistry and Photophysics of Coordination Compounds (Lipari, Italy 1999) S. Campagna, S. Serroni, F. Barigelletti Guest Editors Coord. Chem. Special Issue (2000).
[17] D.J. Stufkens Coord. Chem. Rev. Special Issue Amsterdam 230(2002).
[18] A. Assion, T. Baumert, M. Bergt, T. Brixner, B. Kiefer, V. Seyfried, M. Strehle, G. Gerber, Science 282 (1998) 919.
[19] T.J. Meyer, Pure Applied Chem. 58 (1986) 1193.
[20] M.S. Wrighton, Chem. Rev. 74 (1974) 401.
[21] G.L. Geoffroy, M.S. Wrighton, Organometallic Photochemistry, Academic Press, New York, 1979.
[22] H.B. Schlegel, in: D.R. Yarkony (Ed.), Modern electronic structure theory, World Scientific, Singapore, 1995, pp. 459–500.
[23] U.von Barth, Phys. Rev. A 20 (1979) 1693.
[24] U.von Barth, Phys. Scr. 21 (1980) 585.
[25] C. Daul, H.-U. Güdel, J. Weber, J. Chem. Phys. 98 (1992) 4023.
[26] C. Daul, E.J. Baerends, P. Vernooijs, Inorg. Chem. 33 (1994) 3543.
[27] M. Lannoo, G.A. Baraff, M. Schlüter, Phys. Rev. B 24 (1981) 943.
[28] J.H. Wood, J. Phys. B: At. Mol. Phys. 13 (1980) 1.
[29] E. Runge, E.K.U. Gross, Phys. Rev. Lett. 52 (1984) 997.
[30] E.K.U. Gross, W. Kohn, Adv. Quantum Chem. 21 (1990) 255.
[31] E.K.U. Gross, J.F. Dobson, M. Petersilka, Density Functional Theory, Springer, Heidelberg, 1996.
[32] M.E. Casida, Recent Advances in Density Functional Methods, World Scientific, Singapore, 1995.
[33] C.C.J. Roothan, Rev. Mod. Phys. 23 (1951) 69.
[34] C.C.J. Roothan, J. Chem. Phys. 51 (1960) 363.
[35] B.O. Roos, Chem. Phys. Lett. 15 (1972) 153.
[36] B.O. Roos, P.E.M. Siegbahn, The Direct Configuration Interaction Method from Molecular Integrals, Methods of Electronic Structure Theory, Plenum Press, New York, 1977.
[37] I. Shavitt, The Method of Configuration Interaction, in Methods of Electronic Structure Theory, Plenum Press, New York, 1977.
[38] P.E.M. Siegbahn, Chem. Phys. 25 (1977) 197.
[39] B.O. Roos, The Multiconfigurational (MC) SCF Method, in Methods in Computational Physics, D. Reidel, Dordrecht, 1983.
[40] H.J. Werner, Ab initio Methods in Quantum Chemistry Part II, John Wiley & Sons Ltd, Chichester, 1987, pp. 1–62.
[41] R. Shepard, Ab initio Methods in Quantum Chemistry Part II The Multiconfiguration SCF method, John Wiley & Sons Ltd, Chichester, 1987, pp. 63–200.
[42] H.-J. Werner, P.J. Knowles, J. Chem. Phys. 89 (1988) 5803.
[43] D.C. Comeau, R.J. Bartlett, Chem. Phys. Lett. 207 (1993) 414.
[44] J. Geertsen, M. Rittby, R.J. Bartlett, Chem. Phys. Lett. 164 (1989) 57.
[45] H. Sekino, R.J. Bartlett, Int. J. Quantum Chem. Symp. 18 (1984) 255.
[46] J.F. Stanton, R.J. Bartlett, J. Chem. Phys. 98 (1993) 7029.
[47] J.F. Stanton, R.J. Bartlett, J. Chem. Phys. 98 (1993) 9335.
[48] H. Nakatsuji, Chem. Phys. Lett. 59 (1978) 362.
[49] H. Nakatsuji, Chem. Phys. Lett. 67 (1979) 329.
[50] H. Nakatsuji, Chem. Phys. Lett. 67 (1979) 334.
[51] K. Andersson, P.-A. Malmqvist, B.O. Roos, A.J. Sadlej, K. Wolinski, J. Phys. Chem. 94 (1990) 5483.
[52] K. Andersson, P.A. Malmqvist, B.O. Roos, J. Chem. Phys. 96 (1992) 1218.
[53] K. Andersson, B.O. Roos, P.-A. Malmqvist, P.-O. Widmark, Chem. Phys. Lett. 230 (1994) 391–434.
[54] J. Finley, P.-A. Malmqvist, B.O. Roos, L. Serrano-Andrés, Chem. Phys. Lett. 288 (1998) 299.
[55] MOLCAS 5.0, University of Lund (2000).
[56] GAUSSIAN Carnegie Office Park, Pittsburgh PA, USA, 1998.
[57] H.-J. Werner, P.J. Knowles, R.D. Amos, MOLPRO version 2002.1, 2002.
[58] R.Ahlrichs. al., TURBOMOLE Program Package for ab initio electronic structure calculations version 5.5 Univ. Karlsruhe, Physical Chemist, Karlsruhe, Germany, 2002.
[59] J.F. Stanton, J. Gauss, S.A. Perera, A. Yau, J.D. Watts, M. Nooijen, N. Oliphant, P.G. Szalay, W.J. Lauderdale, S.R. Gwaltney, S. Beck, A. Balkova, D.E. Bernholdt, K.-K. Baeck, P. Rozyczko, H. Sekino, C. Hober, J. Pittner, R.J. Bartlett, ACES II Quantum Theory Project, University of Florida, 2002.
[60] E.J. Baerends, F.M. Bickelhaupt, S.J.A.v. Gisbergen, C.F. Guerra, J.G. Snijders, G. Velde, T. Ziegler, ADF version 2002.21 SCM Theoretical Chemistry, Vrije Universiteit, Amsterdam, The Netherlands, 2002.
[61] M. Dupuis et al., Electronic Structure System HONDO 8.5, 1994.
[62] K.H. Johnson, J.F.C. Smith, Chem. Phys. Lett. 10 (1971) 219.
[63] T. Ziegler, A. Rauk, E.J. Baerends, Theor. Chim. Acta 43 (1977) 261.
[64] C. Daul, Int. J. Quantum Chem. Symp. 52 (1994) 867.
[65] C. Jamorski, M.E. Casida, D.R. Salahub, J. Chem. Phys. 104 (1996) 5134.
[66] M.E. Casida, Recent Advances in Density Functional Methods, World Scientific, Singapore, 1996.
[67] M.E. Casida, in J.M.S. Ed. (Editor), Recent developments and applications of modern DFT, Elsevier Science, Amsterdam, 1996, pp. 391–434.
[68] A. Rosa, E.J. Baerends, S.J.A. Gisbergen, E.V. Lenthe, J.A. Groeneveld, J.G. Snijders, J. Am. Chem. Soc. 121 (1999) 10356.
[69] K. Wakamatsu, K. Nishimito, T. Shibahara, Inorg. Chem. Commun. 3 (2000) 677.
[70] S.J.A.V. Gisbergen, J.A. Groeneveld, A. Rosa, J.G. Snijders, E.J. Baerends, J. Phys. Chem. Sect. A 103 (1999) 6835.
[71] G. Ricciardi, A. Rosa, S.J.A.V. Gisbergen, E.J. Baerends, J. Phys. Chem. Sect. A 104 (2000) 635.
[72] A. Rosa, G. Ricciardi, E.J. Baerends, J.A. van Gisbergen, J. Phys. Chem. Sect. A 105 (2001) 3311.
[73] G. Ricciardi, A. Rosa, E.J. Baerends, J. Phys. Chem. Sect. A 105 (2001) 5242.
[74] M. Turki, C. Daniel, S. Zalis, J.A. Vlcek, J. van Slageren, D.J. Stufkens, J. Am. Chem. Soc. 123 (2001) 11431.
[75] J. Full, L. Gonzalez, C. Daniel, J. Phys. Chem. Sect. A 105 (2001) 184.
[76] M.E. Casida, F. Gutierrez, J. Guan, F.-X. Gadea, D.R. Salahub, J.-P. Daudey, J.Chem. Phys. 113 (2000) 7062.
[77] M.E. Casida, D.R. Salahub, J. Chem. Phys. 113 (2000) 8918.
[78] H. Chermette, Coord. Chem. Rev. 178–180 (1998) 699.
[79] L.G. Vanquickenborne, M. Hendrickx, I. Hyla-Kryspin, L. Haspeslagh, Inorg. Chem. 25 (1986) 885.
[80] M.M. Rohmer, A. Veillard, M.H. Wood, Chem. Phys. Lett. 29 (1974) 466.
[81] I.H. Hillier, J. Kendrick, Inorg. Chem. 15 (1976) 520.
[82] P.J. Hay, J. Am. Chem. Soc. 100 (1978) 2411.
[83] H. Nakatsuji, M. Ehara, M.H. Palmer, M.F. Guest, J. Chem. Phys. 97 (1992) 2561.
[84] B.O. Roos, P.R. Taylor, P.E.M. Siegbahn, Chem. Phys. 48 (1980) 157.
[85] B.O. Roos, in: K.P. Lawley (Ed.), Advances in Chemical Physics; Ab initio methods in quantum chemistry, John Wiley & Sons Ltd, Chichester, 1987, p. 399.
[86] P.-A. Malmqvist, A. Rendell, B.O. Roos, J. Phys. Chem. 94 (1990) 5477.
[87] M.R.D. Hachey, C. Daniel, Inorg. Chem. 37 (1998) 1387.
[88] B.O. Roos, K. Andersson, Chem. Phys. Lett. 245 (1995) 215.

[89] O. Kühn, M.R.D. Hachey, M.M. Rohmer, C. Daniel, Chem. Phys. Lett. 322 (2000) 199.
[90] J. Bossert, N. Ben Amor, A. Strich, C. Daniel, Chem. Phys. Lett. 342 (2001) 617.
[91] J. Cizek, J. Chem. Phys. 45 (1969) 4256.
[92] F. Coester, Nucl. Phys. 7 (1966) 421.
[93] J. Paldus, J. Cizek, I. Shavitt, Phys. Rev. A 5 (1972) 50.
[94] H. Nakatsuji, K. Hirao, J. Chem. Phys. 68 (1978) 2035.
[95] R.J. Bartlett, Ann. Rev. Phys. Chem 32 (1981) 359.
[96] J.D. Watts, J. Gauss, R.J. Bartlett, J. Chem. Phys. 98 (1993) 8718.
[97] N. Oliphant, R.J. Bartlett, J. Am. Chem. Soc. 116 (1994) 4091.
[98] M. Nooijen, V. Lotrich, J. Chem. Phys. 113 (2000) 494.
[99] P. Pulay, in: D.R. Yarkony (Ed.), Modern Electronic Structure Theory, World Scientific, Singapore, 1995, pp. 1191–1240.
[100] R. Shepard, in: D.R. Yarkony (Ed.), Modern electronic structure theory, World Scientific, Singapore, 1995, pp. 345–458.
[101] E.J. Baerends, A. Rosa, Coord. Chem. Rev. 177 (1998) 97.
[102] C.V. Caillie, R.D. Amos, Chem. Phys. Lett. 317 (2000) 159.
[103] T. Kreibich, M. Lein, V. Engel, E.K.U. Gross, Phys. Rev. Lett. 87 (2001) 103901.
[104] T. Kreibisch, E.K.U. Gross, Phys. Rev. Lett. 86 (2001) 2984.
[105] A. Sanchez-Galvez, P. Hunt, M.A. Robb, M. Olivucci, T. Vreven, H.B. Schlegel, J. Am. Chem. Soc. 122 (2000) 2911.
[106] M. Garavelli, B.R. Smith, M.J. Bearpark, F. Bernardi, M. Olivucci, M.A. Robb, J. Am. Chem. Soc. 122 (2000) 5568.
[107] F. Jolibois, M.J. Bearpark, S. Klein, M. Olivucci, M.A. Robb, J. Am. Chem. Soc. 122 (2000) 5801.
[108] E. Fernandez, L. Blancafort, M. Olivucci, M.A. Robb, J. Am. Chem. Soc. 122 (2000) 7528.
[109] S. Wilsey, L. Gonzalez, M.A. Robb, K.H. Houk, J. Am. Chem. Soc. 122 (2000) 5866.
[110] M.C. Heitz, C. Daniel, J. Am. Chem. Soc. 119 (1997) 8269.
[111] D. Guillaumont, A. Vlcek, C. Daniel, J. Phys. Chem. Sect. A 105 (2001) 1107.
[112] R. Schinke, Photodissociation Dynamics, Cambridge University Press, Cambridge, 1993.
[113] E.J. Heller, Acc. Chem. Res. 14 (1981) 368.
[114] U. Wahlgren, B. Schimmelpfennig, S. Jusuf, H. Stromsnes, O. Gropen, L. Maron, Chem. Phys. Lett. 525 (1998) 2987.
[115] B.A. Hess, Phys. Rev. A 33 (1986) 3742.
[116] G. Jansen, B.A. Hess, Phys. Rev. A 39 (1989) 6016.
[117] O.D. Häberlen, N. Rösch, Chem. Phys. Lett. 199 (1992) 491.
[118] N. Rösch, S. Krüger, M. Mayer, V.A. Nasluzov, Theoretical and Computational Chemistry, Amsterdam, 1996, p. 497.
[119] PARAGAUSS N. Rösch.et al. Technische Universität, Munich, 1999.
[120] G.T. Velde, F.M. Bickelhaupt, E.J. Baerends, C.F. Guerra, S.J.A.v. Gisbergen, J.G. Snijders, T. Ziegler, J. Comp. Chem. 22 (2001) 931.
[121] E. van Lenthe, E.J. Baerends, J.G. Snijders, Chem. Phys. 99 (1993) 4597.
[122] E. van Lenthe, E.J. Baerends, J.G. Snijders, Chem. Phys. 101 (1994) 9783.
[123] D. Andrae, U. Häussermann, M. Dolg, H. Stoll, H. Preuss, Theor. Chim. Acta 77 (1990) 123.
[124] P.J. Hay, W.R. Wadt, J. Chem. Phys. 82 (1985) 270.
[125] P.J. Hay, W.R. Wadt, J. Chem. Phys. 82 (1985) 299.
[126] M.M. Hurley, L.F. Pacios, P.A. Christiansen, R.B. Ross, W.C. Ermler, J. Chem. Phys. 84 (1986) 6840.
[127] W. Küche, M. Dolg, H. Stoll, H. Preuss, Mol. Phys. 74 (1991) 1245.
[128] L.A. LaJohn, P.A. Christiansen, R.B. Ross, T. Atashroo, W.C. Ermler, J. Chem. Phys. 87 (1987) 2812.
[129] R.B. Ross, J.M. Powers, T. Atashroo, W.C. Rmler, L.A. LaJohn, P.A. Christiansen, J. Chem. Phys. 93 (1990) 6654.
[130] W.J. Stevens, M. Krauss, H. Basch, P.G. Jasien, Can. J. Chem. 70 (1992) 612.
[131] Z. Barandiaran, L. Seijo, Can. J. Chem. 70 (1992) 409.
[132] M. Casarubios, L. Seijo, J. Mol. Struct. (THEOCHEM) 59 (1998) 426.
[133] M. Casarubios, L. Seijo, J. Chem. Phys. 110 (1999) 784.
[134] L. Seijo, J. Chem. Phys. 102 (1995) 8078.
[135] T. Saue, V. Bakken, T. Enevoldsen, T. Helgaker, H.J.A. Jensen, J.K. Laerdahl, K. Ruud, J. Thyssen, L. Visscher, DIRAC Release 3.2, 2000.
[136] L. Visscher, O. Visser, H. Aerts, H. Merenga, W.C. Nieuwpoort, Chem. Phys. Chem. 81 (1994) 120.
[137] T. Nakajima, K. Hirao, Chem. Phys. Lett. 302 (1999) 383.
[138] T. Nakajima, K. Hirao, J. Chem. Phys. 113 (2000) 7786.
[139] T. Yanai, T. Nakajima, Y. Ishikawa, K. Hirao, J. Chem. Phys. 114 (2001) 6525.
[140] T. Yanai, H. Iikura, T. Nakajima, Y. Ishikawa, K. Hirao, J. Chem. Phys. 115 (2001) 8267.
[141] H.M. Quiney, H. Skaane, I. Grant, Adv. Quantum Chem. 32 (1999) 1.
[142] K.G. Dyall, P.R. Taylor, K.Faegri. Jr., H. Partridge, J. Chem. Phys. 95 (1991) 2583.
[143] L. Visscher, W.C. Nieuwport, Theor. Chim. Acta 88 (1994) 447.
[144] C. Daniel, D. Guillaumont, C. Ribbing, B. Minaev, J. Phys. Chem. Sect. A 103 (1999) 5766.
[145] M. Kleinschmidt, J. Tatchen, C.M. Marian, J. Comp. Chem. 23 (2002) 824.
[146] K. Pierloot, B. Dumez, P.-O. Widmark, B.O. Roos, Theor. Chim. Acta 90 (1995) 87.
[147] R. Pou-Amerigo, M. Merchan, I. Nebot-Gill, P.-O. Widmark, B.O. Roos, Theor. Chim. Acta 92 (1995) 149.
[148] H. Johansen, S. Rettrup, Mol. Phys. 49 (1983) 1209.
[149] M. Atanasov, T.C. Brunold, H.U. Güdel, D. Daul, Inorg. Chem. 37 (1998) 4589.
[150] P. Boulet, H. Chermette, C. Daul, F. Gilardoni, F. Rogemond, J. Weber, G. Zuber, J. Phys. Chem. Sect. A 105 (2001) 885.
[151] H. Nakai, Y. Ohmari, H. Nakatsuji, J. Chem. Phys. 95 (1991) 8287.
[152] Y.S. Sohn, D.N. Hendrickson, H.B. Gray, J. Am. Chem. Soc. 93 (1971) 3603.
[153] M. Kotzian, N. Rösch, H. Schröder, M.C. Zerner, J. Am. Chem. Soc. 111 (1989) 7687.
[154] K. Pierloot, E. Tsokos, L.G. Vanquickenborne, J. Phys. Chem. 100 (1996) 16545.
[155] N.A. Beach, H.B. Gray, J. Am. Chem. Soc. 90 (1968) 5731.
[156] L.G. Vanquickenborne, J. Verhulst, J. Am. Chem. Soc. 105 (1983) 1769.
[157] K. Pierloot, J. Verhulst, P. Verbeke, L.G. Vanquickenborne, Inorg. Chem. 28 (1989) 3059.
[158] C. Pollak, A. Rosa, E.J. Baerends, J. Am. Chem. Soc. 121 (1997) 10356.
[159] T.J. Meyer, J.V. Caspar, Chem. Rev. 85 (1985) 187.
[160] R.A. Levenson, H.B. Gray, J. Am. Chem. Soc. 97 (1975) 6042.
[161] A. Rosa, G. Ricciardi, E.J. Baerends, D.J. Stufkens, Inorg. Chem. 34 (1995) 3425.
[162] K. Pierloot, J.O.A.D. Kerpel, U. Ryde, B.O. Roos, J. Am. Chem. Soc. 119 (1997) 218.
[163] K. Pierloot, J.O.A.D. Kerpel, U. Ryde, M.H.M. Olsson, B.O. Roos, J. Am. Chem. Soc. 120 (1998) 13156.
[164] L.B. LaCroix, S.E. Shadle, Y. Wang, B.A. Averill, B. Hedman, K.O. Hodgson, E.I. Solomon, J. Am. Chem. Soc. 118 (1996) 7755.
[165] W. Jentzen, I. Turowska-Tyrk, W.R. Scheidt, J.A. Schellnut, Inorg. Chem. 35 (1996) 3559.
[166] L. Edwards, M. Gouterman, Mol. Spectrosc. 33 (1970) 292.
[167] D.J. Stufkens, Comments Inorg. Chem. 13 (1992) 359.

[168] M.P. Aarnts, M.P. Wilms, K. Peleen, J. Fraanje, K. Goubitz, G. Hartl, D.J. Stufkens, E.J. Baerends, J.A. Vlcek, Inorg. Chem. 35 (1996) 5468.
[169] M.P. Aarnts, D.J. Stufkens, M.P. Wilms, E.J. Baerends, J.A. Vlcek, I.P. Clark, M.W. George, J.J. Turner, Chem. A Eur. J. 2 (1996) 1556.
[170] H.A. Nieuwenhuis, D.J. Stufkens, A. Oskam, Inorg. Chem. 33 (1994) 3212.
[171] H.A. Nieuwenhuis, D.J. Stufkens, A. Oskam, J.A. Vlcek, Inorg. Chem. 34 (1995).
[172] H.A. Nieuwenhuis, D.J. Stufkens, R.-A. McNicholl, A.H.R. Al-Obaidi, C.G. Coates, S.E.J. Bell, J.J.M. Garvey, J. Westwell, M.W. George, J.J. Turner, J. Am. Chem. Soc. 117 (1995) 5579.
[173] A. Rosa, G. Ricciardi, E.J. Baerends, D.J. Stufkens, Inorg. Chem. 35 (1996) 2886.
[174] S.K. Kim, S. Pedersen, A.H. Zewail, Chem. Phys. Lett. 233 (1995) 500.
[175] M. Turki, C. Daniel, to be published (2002).
[176] S. Villaume, C. Daniel, to be published (2002).
[177] I. Bruand-Cote, C. Daniel, Chem. A Eur. J. 8 (2002) 1361.
[178] D. Guillaumont, C. Daniel, J. Am. Chem. Soc. 121 (1999) 11733.
[179] C.J. Kleverlaan, D.M. Martino, H.v. Willigen, D.J. Stufkens, A. Oskam, J. Phys. Chem. 100 (1996) 18607.
[180] C.J. Kleverlaan, D.J. Stufkens, I.P. Clark, M.W. George, J.J. Turner, D.M. Martino, H. vanWilligen, J.A. Vlcek, J. Am. Chem. Soc. 120 (1998) 10871.
[181] C.J. Kleverlaan, D.J. Stufkens, Inorg. Chim. Acta 284 (1999) 61.
[182] B.D. Rossenaar, E. Lindsay, D.J. Stufkens, J.A. Vlcek, Inorg. Chim. Acta 250 (1996) 5.
[183] B.D. Rossenaar, D.J. Stufkens, A. Oskam, J. Fraanje, K. Goubitz, Inorg. Chim. Acta 247 (1996) 215.
[184] I.H. Hillier, V.R. Saunders, Chem. Phys. Lett. 9 (1971) 219.
[185] L. Holt, C.J. Balhausen, Theor. Chim. Acta 7 (1967) 313.
[186] G.M. Bancroft, E. Pellach, J.S. Tee, Inorg. Chem. 21 (1982) 2950.
[187] Y.S. Sohn, D.N. Hendrickson, H.B. Gray, J. Am. Chem. Soc. 93 (1971) 3603.